Supplemental Information for

MicroRNA-122 plays a critical role in liver homeostasis and hepatocarcinogenesis

Dr. Ann-Ping Tsou
Department of Biotechnology and Laboratory Science in Medicine
National Yang-Ming University, Taipei 112, Taiwan, ROC.
Telephone: (886)-2-28267155
Facsimile: (886)-2-28264092
Email: aptsou@ym.edu.tw

Materials and Methods

RNA isolation, high-density oligonucleotide microarray analysis and expression validation. The microarray hybridizations were performed using total RNA prepared from the liver samples of three wild-type mice and four *Mir122a*$^{-/-}$ mice at an age of 2-months, liver samples from two wild-type mice and tumor samples from three *Mir122a*$^{-/-}$ mice at an age of 11-months, liver samples from three wild-type mice and tumor samples from five *Mir122a*$^{-/-}$mice at an age of 14-months. Super RNApure (Geneisis Biotech Inc) was used to extract total RNA from the frozen liver samples. GeneChip Mouse Genome 430 2.0 Affymetrix oligonucleotide Gene Chips (Affymetrix) were analyzed at Microarray & Gene Expression Analysis Core Facility (VGH-YM Genome Center, National Yang-Ming University) according to the Affymetrix protocols. The arrays were scanned using an Affymetrix GeneChip scanner 3000. The resulting image data was captured and saved in CEL file format using GeneChip Operating Software v.1.4.0.036. CEL files were imported into Partek Genomic Suite (version 6.5) with probeset intensity normalized using the robust multi-array analysis (RMA). All the data files are presented in compliance with MIAMI guidelines and can be accessed online at the Gene Expression Omnibus (series accession numbers GSE27713 and GSE31453). Microarray dataset was analyzed using the Gene Set Enrichment Analysis (GSEA, Version 3.2) from Broad Institute (37). For GSEA analysis, probesets were collapsed to genes using median values and then ranked with the Signal2Noise method. The following three comparisons were made: 2-month *Mir122a*$^{-/-}$ versus wild-type, 11-month *mir-122*$^{-/-}$ tumor versus 11-month wild-type

livers and 14-month *Mir122a*$^{-/-}$ tumor versus 14-month wild-type livers. A total of 203 gene sets, including 197 gene sets from KEGG pathway database, 1 gene set from the BioCarta database, and 5 custom curated gene sets, were included in the enrichment analysis. Genes included in the "fibrogenic factor" gene set were curated (39, 63, 64). Differentially expressed genes in mice treated with LNA-anti-miR-122 for 1 week were used to produce the "LNA-MIR-122-1W_UP" and "LNA-MIR-122-1W_DN" gene sets (38). Genes differentially expressed in human HCC patients with high and low *MIR122* were used to generate the "MIR-122-LVH_UP" and "MIR-122-LVH_DN" gene sets (16). Expression analysis of *Mir122a* was done by TaqMan®MicroRNA Assay (Applied Biosystems). Gene expression was detected by quantitative real-time polymerase chain reaction (qRT-PCR) using the SYBR Green I protocol (Bio-Rad). All values were normalized against beta-2 microglobulin (B2m) mRNA. The primer sequences are listed in Supplemental Table 2.

Identifying Mir122a targets among the up-regulated genes of Mir122a$^{-/-}$ *livers.* Three computational tools, namely miRanda (58), TargetScanS (59) and RNAhybrid (60), which have been successfully integrated by us in miRNAMap previously (61); these were used in this study. In order to achieve higher prediction accuracy, we also integrated another tool, PITA (62). The integrated tools were then used to identify the *MIR122* target sites located within the accessible regions of 3'-UTR of up-regulated genes in the *Mir122a*$^{-/-}$ mouse liver. Up-regulated orthologous genes with target sites in both the mouse and human genomes were pinpointed. The predictive parameters of each miRNA target prediction tool were optimized to yield a better set

of miRNA target candidates (Supplemental Table 8). Furthermore, we recalculated the miRNA/target duplex score using the following single-position base-pairing values. A score of +5 was assigned for G:C and A:U pairs, +2 for G:U wobble pairs, and −3 for mismatch pairs, and the gap-open and gap-elongation parameters were set to −8.0 and −2.0, respectively. The match value s(i) is multiplied by a position specific weight w(i). The position specific weights emphasize the importance of the 'seed region' generally defined as the position 2-8 of the miRNA 5'-end. Thus the total score S for a particular alignment is $S = \sum_{i=1}^{n} w(i) \times s(i)$. A higher score indicates a more stable miRNA/target duplex. In the end 252 up-regulated orthologous genes, which were identified by at least three target prediction tools, were selected for experimental validation and further analysis (Supplemental Table 6).

Performance evaluation. In order to evaluate the performance of the miRNA target prediction tools and our proposed method, we collected 76 experimentally validated *MIR122* target genes and 20 miRNA non-target genes (Supplemental Table 7). This dataset is based on our validated *MIR122* targets and was complemented by additional validated targets curated from miRTarBase. Before the comparing prediction accuracy of the target prediction tools and our proposed method, the parameters used by miRanda and RNAhybrid were optimized. The miRanda score was adjusted from 100 to 180 using step=5 and MFE was set from -10 kcal/mol to -30 kcal/mol with step=-2 kcal/mol. Furthermore, RNAhybrid MFE was adjusted from -10 kcal/mol to -30 kcal/mol with step=-2 kcal/mol. The predictive parameters of TargetScanS and PITA were set at their default values. The optimal parameters of each target prediction tool were

determined by the maximizing the performance (PERF) using the following formula:

$$PERF = Sensitivity(SENS) \times Specificity(SPEC); SENS = \frac{TP}{TP + FN}; SPEC = \frac{TN}{FP + TN}$$

In the equation, TN represents true negative, TP true positive, FN false negative and FP false positive. The MFE threshold of the miRNA and target duplex was -7 kcal/mol and the miRanda score cutoff was specified as 120. The MFE threshold of the miRNA and target duplex in RNAhybrid was set at -23 kcal/mol. The performances of the individual prediction tools and our combinatory method are displayed in Supplemental Table 8. We found that miRanda gave the highest sensitivity, while TargetScanS has the highest specificity. It can be seen that our combinatory method is the best approach to the identification of *Mir122a* targets.

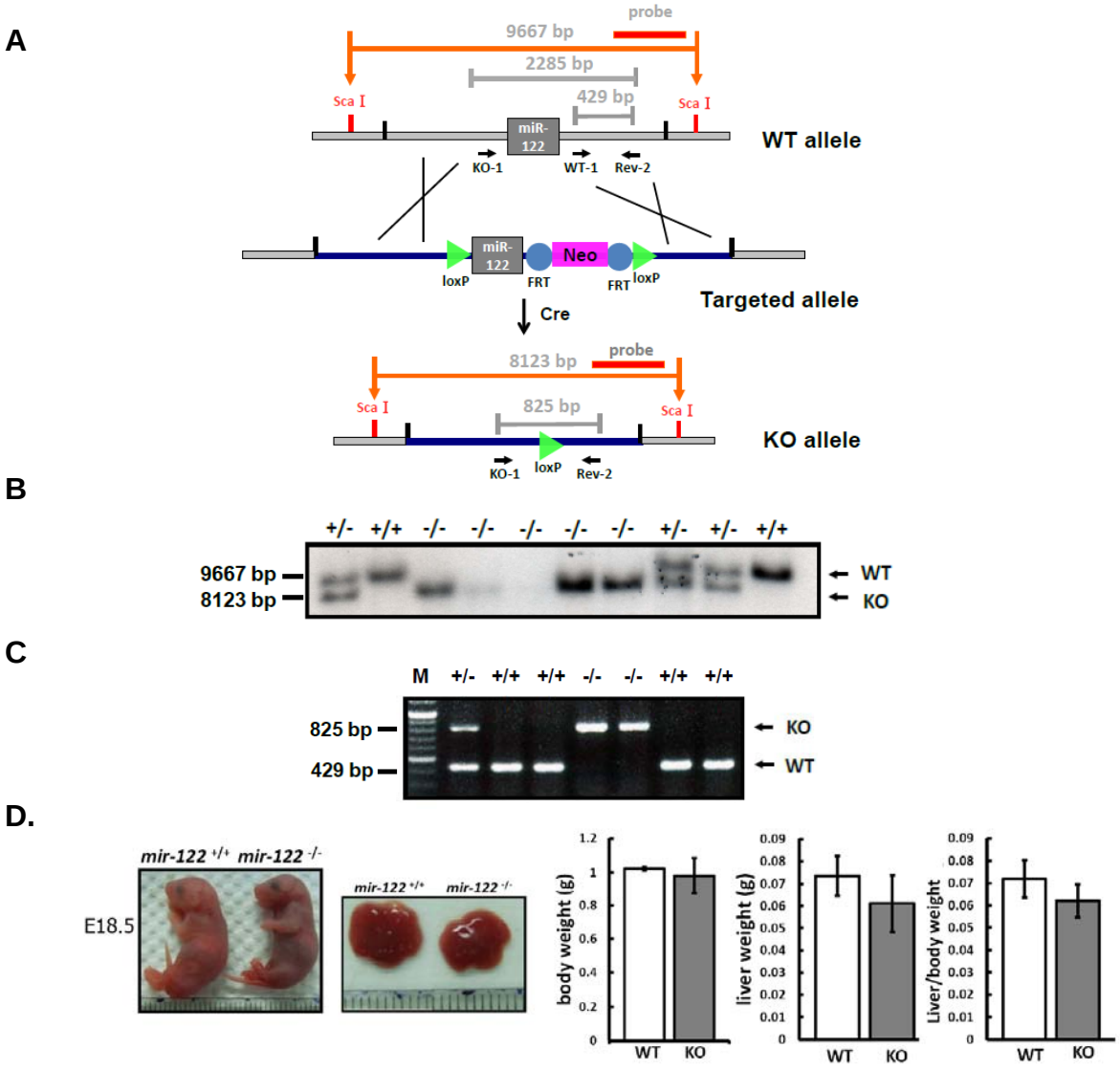

Supplemental Figure 1. Generation of *Mir122a* deletion mice. (A) The strategy for generating *Mir122a* deletion mice by homologous recombination. The BAC clone bMQ-418A13 (chr18: 65269984-65437465) containing the entire *pri-Mir122a* locus was purchased from Geneservice. A genomic fragment of 13 kb encompassing 7.8 kb upstream and 5.1 kb downstream of *pre-Mir122a* was cloned to PL253 in bacterial strain EL350 by the recombineering-based method (19). The genomic fragment of *Mir122a* constructed in PL253 was used to replace the wild-type allele of *Mir122a* in 129Sv mouse embryonic stem cells (MESC). MESC clones containing the targeted allele were identified by Southern blot analysis. Several clones were isolated and transfected with a vector encoding the Cre recombinase to delete a fragment of 1,544 bp containing the entire *pre-Mir122a*. Clones with the *Mir122a* knockout allele were identified by Southern blot analysis and injected into the C57BL/6J blastocysts. Germline transmission of the *Mir122a*$^{-/-}$ allele was achieved by crossing the chimeric mice with normal C57BL/6 mice. The homozygous *Mir122a*$^{-/-}$ mice were generated with littermates from the intercross of the heterozygous mice. **(B)** Genotyping of F1 and successive progenies was performed by Southern blotting with ScaI digested DNA. WT, 9667 bp; homozygous deletion of *Mir122a,* 8123 bp. **(C)** Genotyping with genomic PCR. WT, 429 bp; *Mir122a*$^{-/-}$, 825 bp. **(D)** E18.5 embryos of *Mir122a*$^{-/-}$ and WT mice. Both the body weight and liver weight of the *Mir122a*$^{-/-}$ E18.5 embryos seem to be smaller than that of WT but the differences are not significant. The litter size of *Mir122a*$^{-/-}$ mice is also not significantly different from that of the WT. n=3 mice per group.

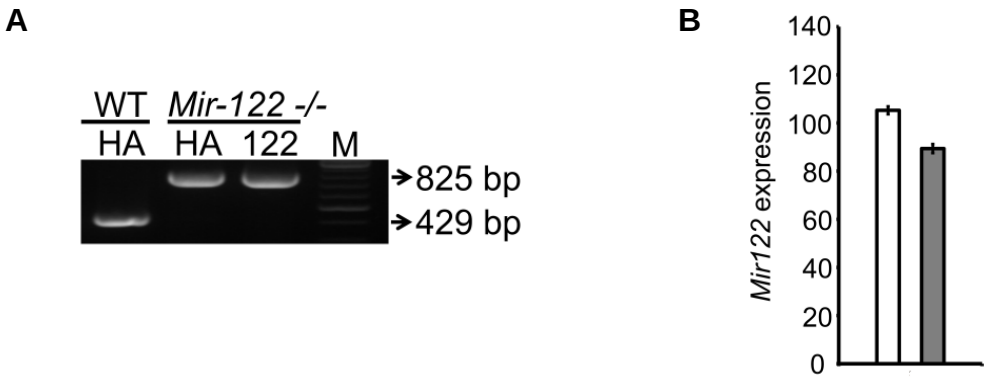

Supplemental Figure 2. Restoration of *Mir122a* in *Mir122a*$^{-/-}$ mice by hydrodynamic injection. All the mice received two hydrodynamic injections, one on day 1 and one on day 15 of 20 μg of plasmid DNA of either the endotoxin-free pcDNA3.1-HA (HA) or pcDNA3.1-HA-*MIRR-122* (122). (WT: HA, □; *Mir122a*$^{-/-}$: 122, ■). **(A)** Genotyping with genomic PCR. WT, 429 bp; *Mir122a*$^{-/-}$, 825 bp. **(B)** Relative high level expression of *Mir122a* in the *Mir122a*$^{-/-}$ livers was detected by qRT-PCR. The genotyping and expression analysis of *Mir122a* were performed one month after injection.

A

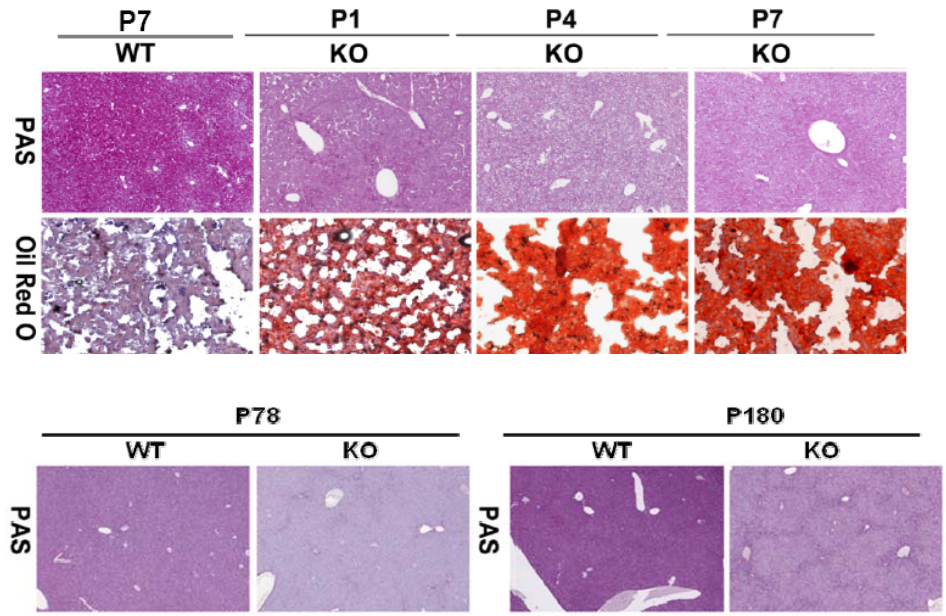

B

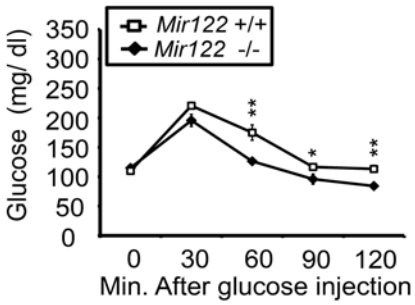

C

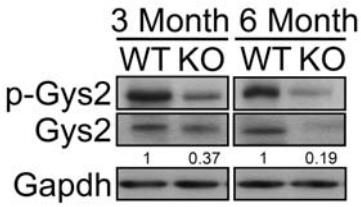

Supplemental Figure 3. Loss of *Mir122a* leads to abnormal glucose metabolism. (A) Pathological features of fatty accumulation (Oil Red O) and reduced glycogen storage (PAS) and developed early in the new born *Mir122a*$^{-/-}$ mice. P1, P4, P7, P78 and P180 are postnatal 1 day, 4 days, 7 days, 78 days and 180 days, respectively. **(B)** *Mir122a*$^{-/-}$ mice had slightly higher glucose levels as shown in the glucose tolerance test. **P* < 0.05, ***P*<0.01. **(C)** Both phosphorylation and the protein level of hepatic glycogen synthase (Gys2) were reduced in the *Mir122a*$^{-/-}$ livers.

A.

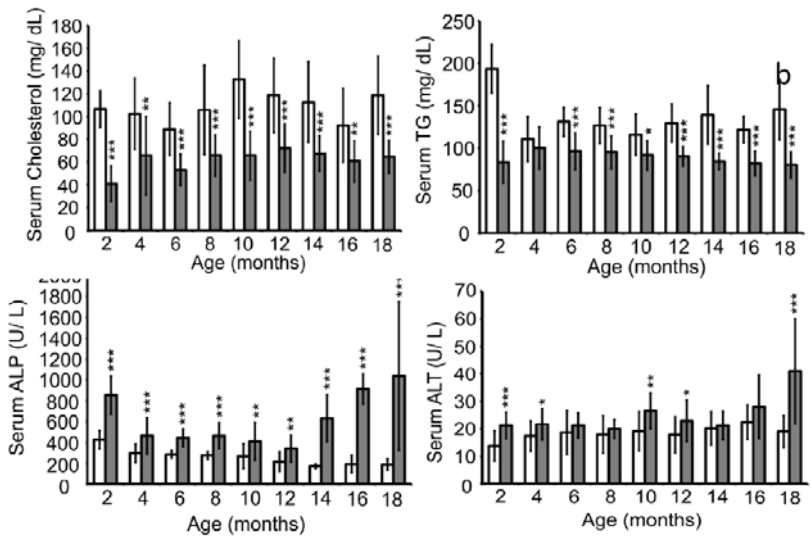

B.

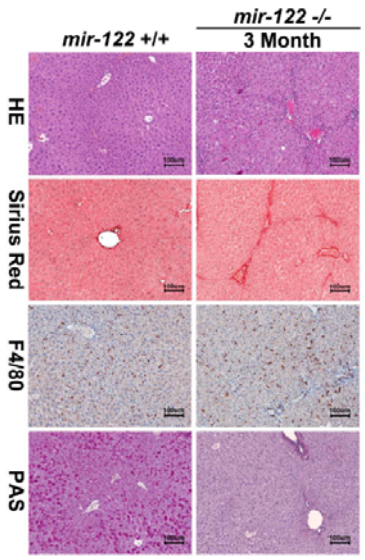

C.

Age	IL-6 level (pg/ ml) WT	KO	Tumor size (mm^3)
12M	0±0	3.4±5.9	0
14M	2±2.7	6.3±3.2	0
16M	2.6±3.1	7.4±5	0
18M	1.6±2.8	7±12.1	0

Age	IL-6 level (pg/ ml) WT	KO	Tumor size (mm^3)
14M	1.4±2.3	4.4±0.49	2.3±2.3
16M	2.9±5.2	7.4±4.95	10.1±9.32
18M	1.6±2.8	19.7±9.29	40.7±14.7
19M	2.1±3.7	78±20.42	368.4±62.1

D.

Age	IL-6 level (pg/ ml) WT	KO	Tumor size (mm^3)
3M	0.1±2.9	0.7±0.6	0
6M	0.5±3.8	0.4±0.5	0
16M	6.4±2.9	17.3±8.2	116±95
18M	3.6±3.8	181.2±270.3	1977.3±1689.6

Supplemental Figure 4. Pathophysiology of female *Mir122a*$^{-/-}$ mice. (A) Serum profile of female *mir-122*$^{-/-}$ mice. Total serum cholesterol, fasting triglyceride (TG), alkaline phosphatase (ALP) and alanine aminotransferase (ALT) were measured enzymatically on a DRI-CHEM3500S autoanalyzer (FUJIFILM). n=20 mice per group. Female *Mir122a*$^{-/-}$ mice (■) exhibited similar serum profiles (low cholesterol/triglyceride and high ALP/ALT) as found in the male *Mir122a*$^{-/-}$ mice (Figure. 1A of the Text). (**B)** Female *Mir122a*$^{-/-}$ mice developed hepatic fibrosis (Sirius Red), inflammation (F4/89 for Kupffer cells) and accumulated less glycogen (PAS staining) as seen in the male mutant mice (Figure 1 of the Text). **(C, D)** Very low level of IL-6 was detected in the WT of both genders. **(C)** Low level of serum IL-6 was detected in the female *Mir122a*$^{-/-}$ mice that are tumor-free (*Upper panel*) but significantly elevated levels of serum IL-6 were detected in the tumor-bearing female *Mir122a*$^{-/-}$ mice (*Lower panel*). **(D)** Similar results were found in the male *Mir122a*$^{-/-}$ mice. There is a clear correlation between the serum IL-6 level and the tumor incidence as well as the tumor volume in both genders of *Mir122a*$^{-/-}$ mice. Serum levels of IL-6 were measured by ELISA. n=5 mice per group. Tumor volume = 0.4*L*W^2.

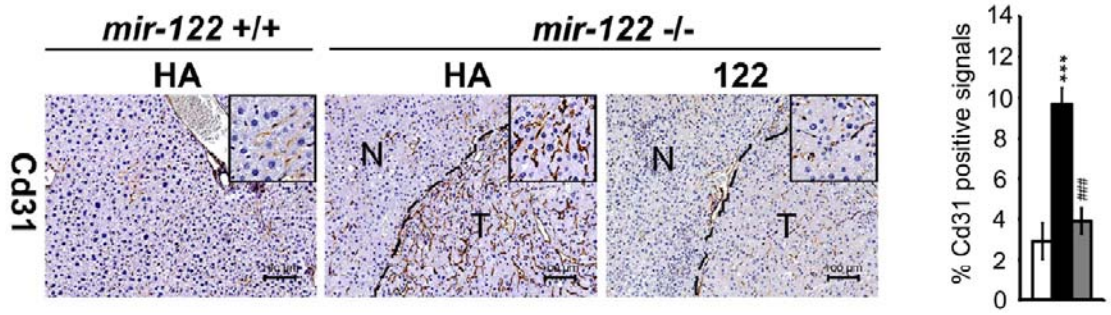

Supplemental Figure 5. Blood vessel distributions of the tumors as revealed by immunohistochemistry staining using the Cd31 antibody. Twenty micrograms of pcDNA3.1-HA (HA) were delivered into the tail veins of WT mice (*122*$^{+/+}$-HA,□), pcDNA3.1-HA to the *Mir122a*$^{-/-}$ mice (*122*$^{-/-}$-HA,■) and pcDNA3.1-HA-*MIR122* to the *Mir122a*$^{-/-}$ mice (*122*$^{-/-}$-122,▩) by hydrodynamic injection for a period of 8 months. ***Left,*** Immunohistochemistry. The dotted lines show the edges of the normal liver area (N) and tumor area (T). Scale bars: 100 μm. ***Right,*** Bar chart shows comparisons of the mean Cd31 positive vessel numbers per high power field of the various tissue sections. Significant reductions in the number of Cd31 positive blood vessels were found for the tumors of the *122*-restored mutant mice groups (▩) compared to the tumors of the control HA-plasmid injected mutant mice group (■). Microvessels that stained positively with the anti-Cd31 antibody were counted in 10 different microscopic fields at 200x using the Aperio Positive Pixel Count v9 software. Due to the small size of the mass, only 2 to 4 fields were counted for the *122*$^{-/-}$-122 tumors. The mean value of the fields was calculated to provide a mean microvessel density. n=3 for *122*$^{+/+}$-HA; n=2 for *122*$^{-/-}$-HA and *122*$^{-/-}$-122.

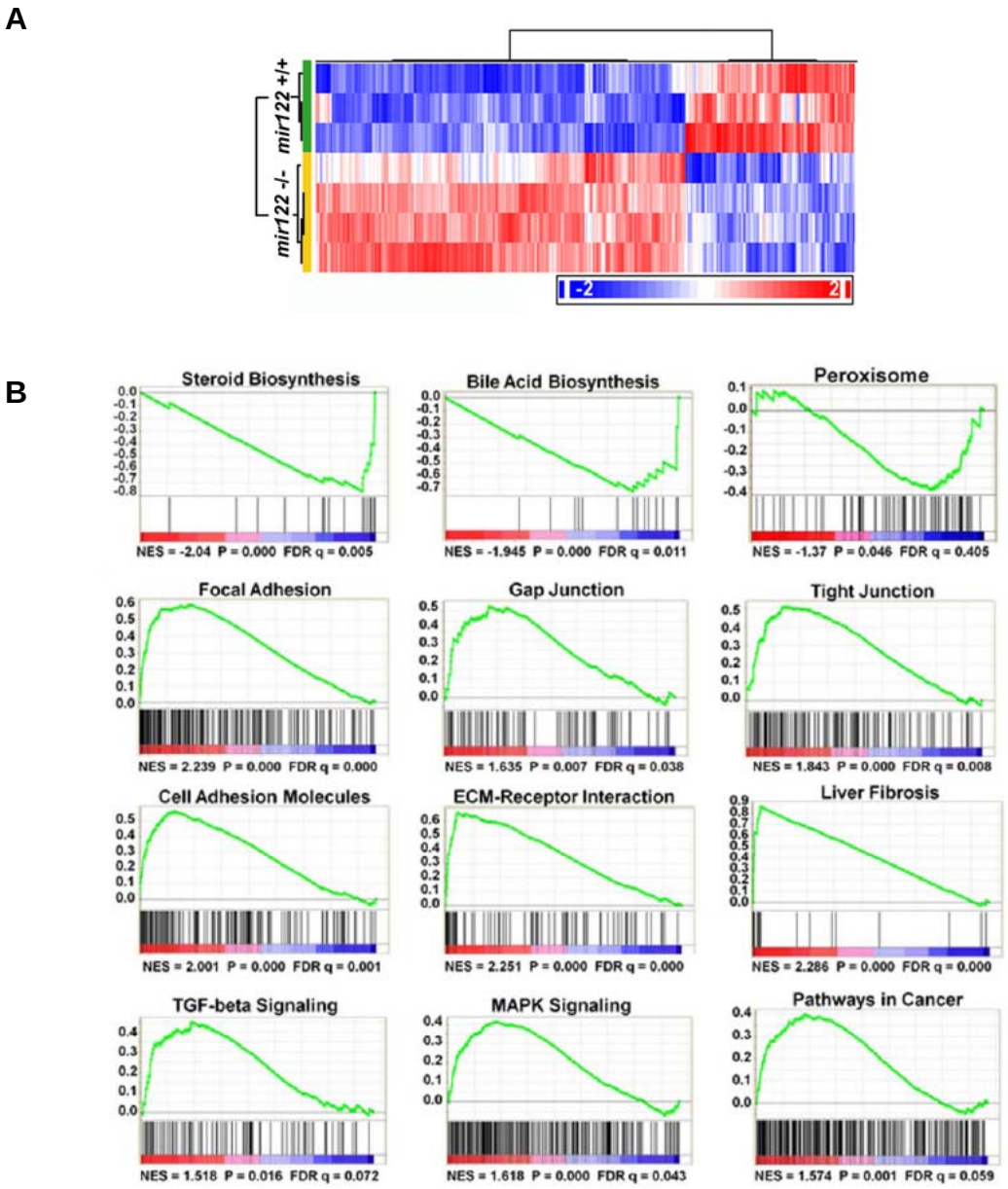

Supplemental Figure 6. *Mir122a* deletion changes the global gene expression. (A) Heat map of the 886 genes that were differentially expressed in the livers of 2-month-old male *Mir122a*$^{-/-}$ and WT mice (cutoff 1.5). The heat scale at the bottom of the map represents changes on a linear scale. Red and blue colors denote up-regulated and down-regulated expressions, respectively. **(B)** GSEA (Gene set enrichment analysis). Enrichment plots of the top three pathways significantly de-enriched in the *Mir122a*$^{-/-}$ mice. Enrichment plots of the significantly up-regulated pathways in the *Mir122a*$^{-/-}$ mice, cell communication (Focal adhesion, Gap junction, Tight junction), cell-cell interaction (Cell adhesion molecules, ECM-receptor interaction), fibrogenic pathways (Liver fibrosis and TGF-beta signaling), signal transduction (MAPK signaling) and major cancer-related phenotypes. NES, normalized enrichment score with the positive and negative scores indicating enrichment and de-enrichment in *Mir122a*$^{-/-}$, respectively. FDR, false detection rate. p, nominal p value. The complete results of the GSEA analysis are listed in Supplemental Table 4.

A

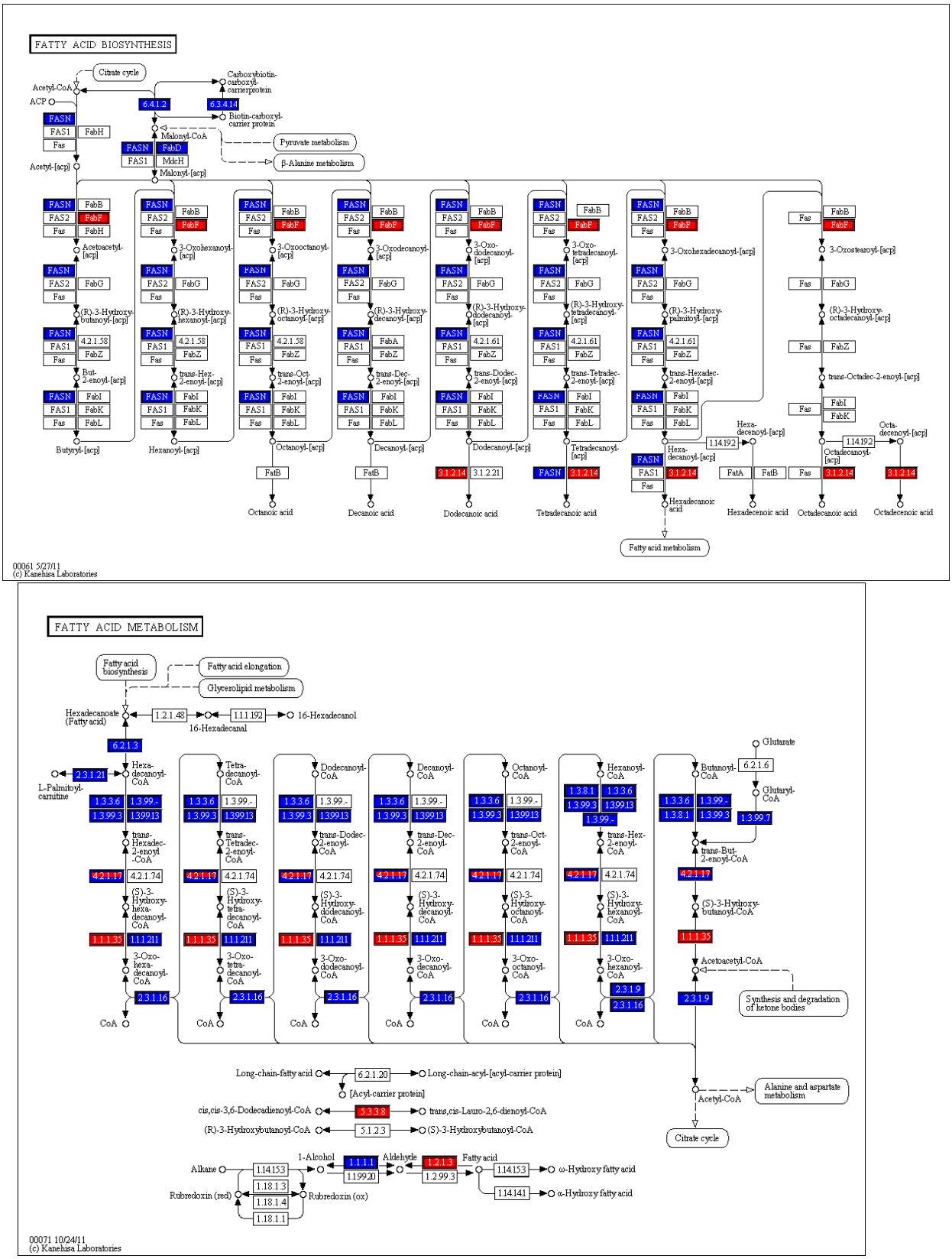

Supplemental Figure 7. The metabolic pathways analyses using KEGG database. (A) Fatty acid biosynthesis (Upper panel) and Fatty acid metabolism (Lower panel), **(B)** Oxidative phosphorylation, **(C)** Peroxisome functions, **(D)** Steroid biosynthesis, **(E)** Primary bile acid biosynthesis, and **(F)** Steroid hormone biosynthesis. Red and blue colors denote up-regulated and down-regulated expressions, respectively.

B.

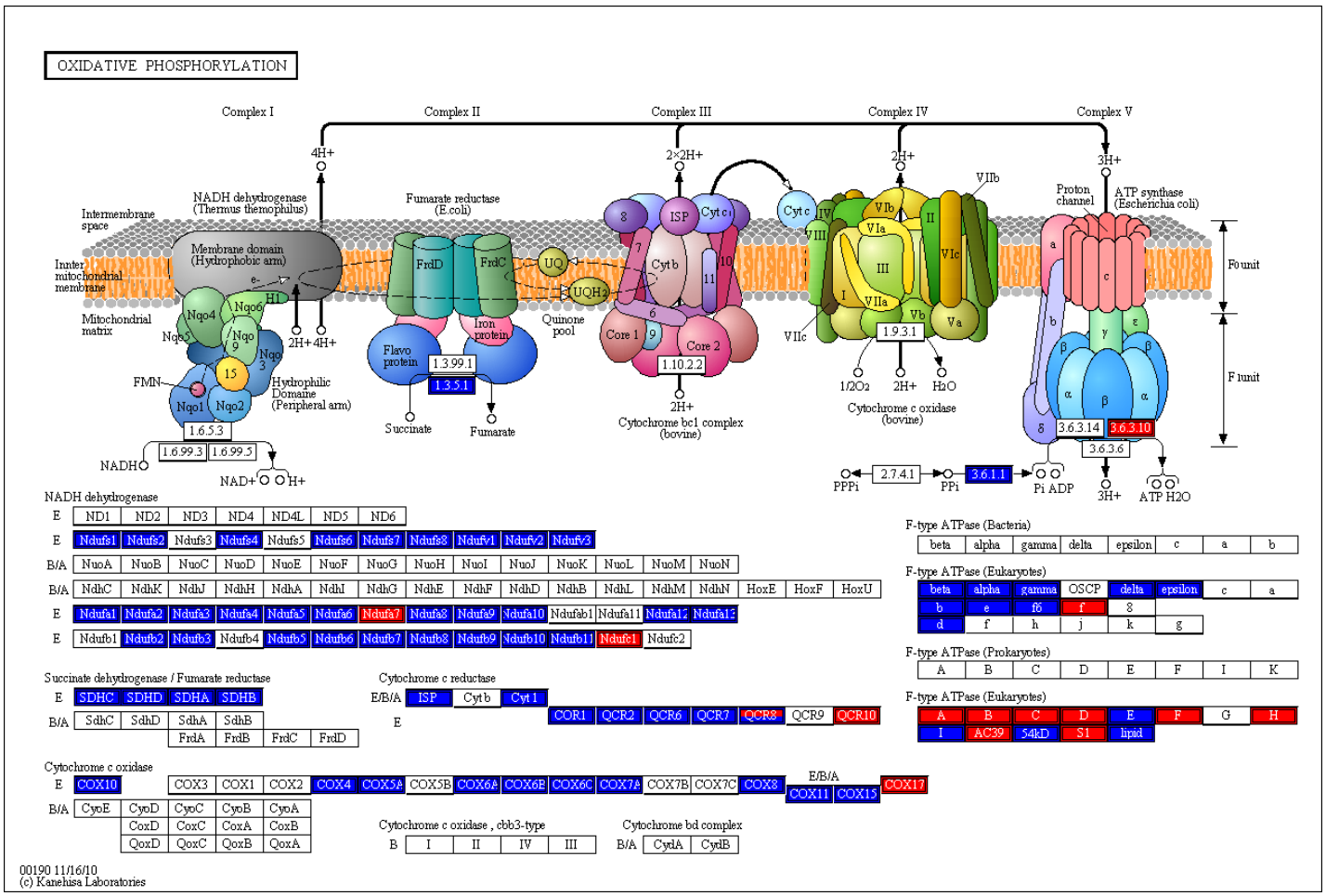

Supplemental Figure 7. (B) Oxidative phosphorylation.

C.

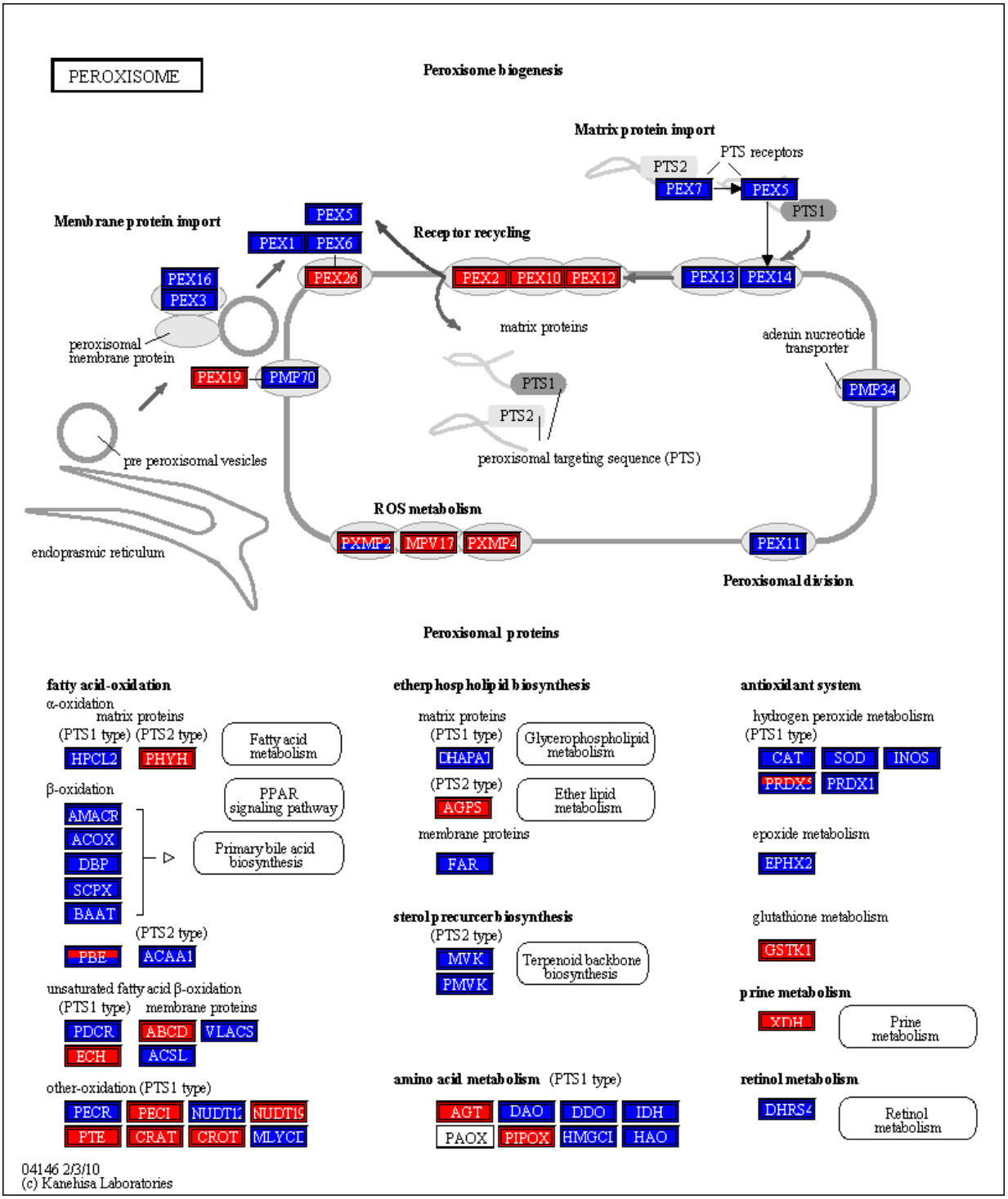

Supplemental Figure 7. (C) Peroxisome functions.

D.

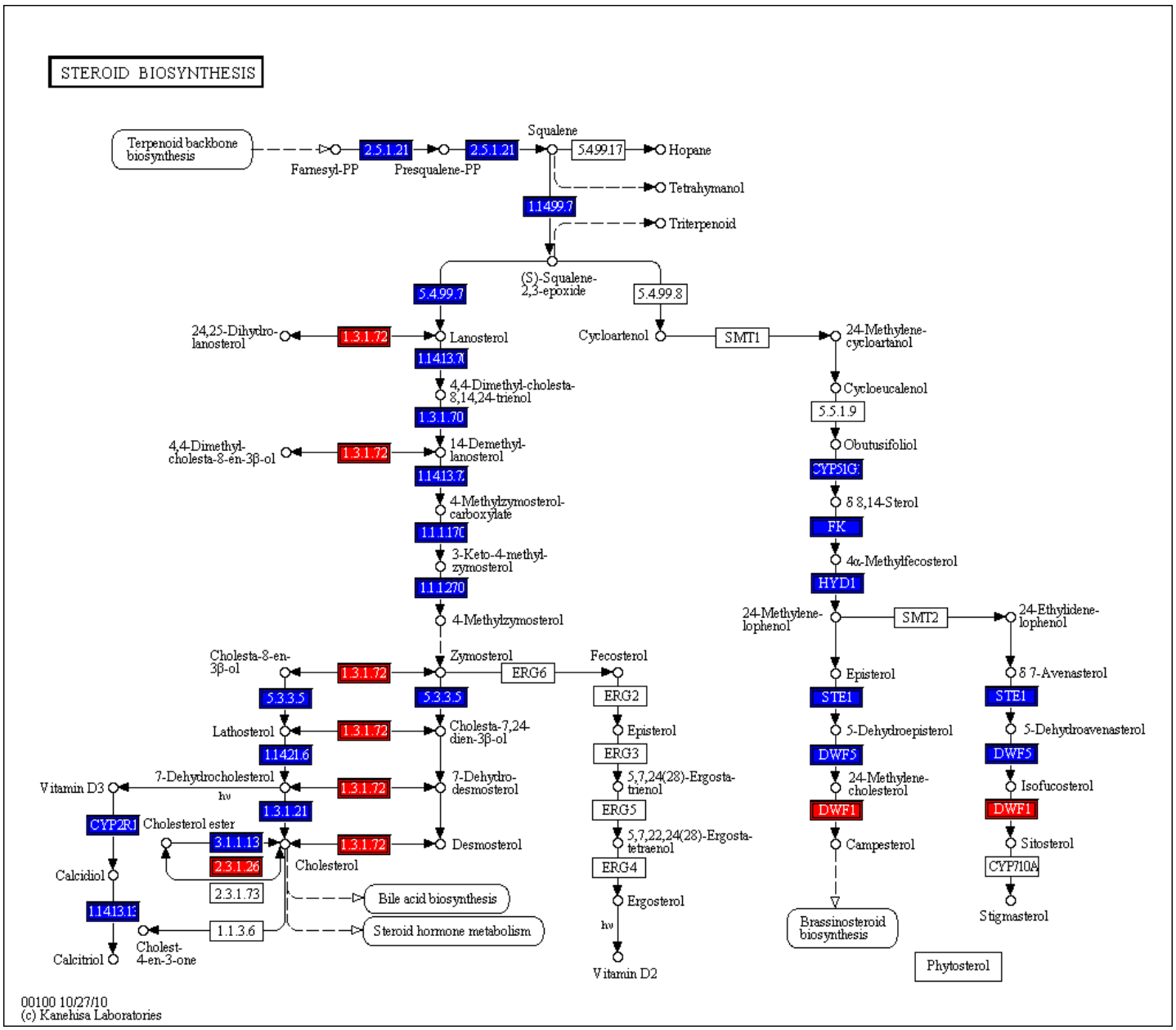

Supplemental Figure 7. (D) Steroid biosynthesis.

E.

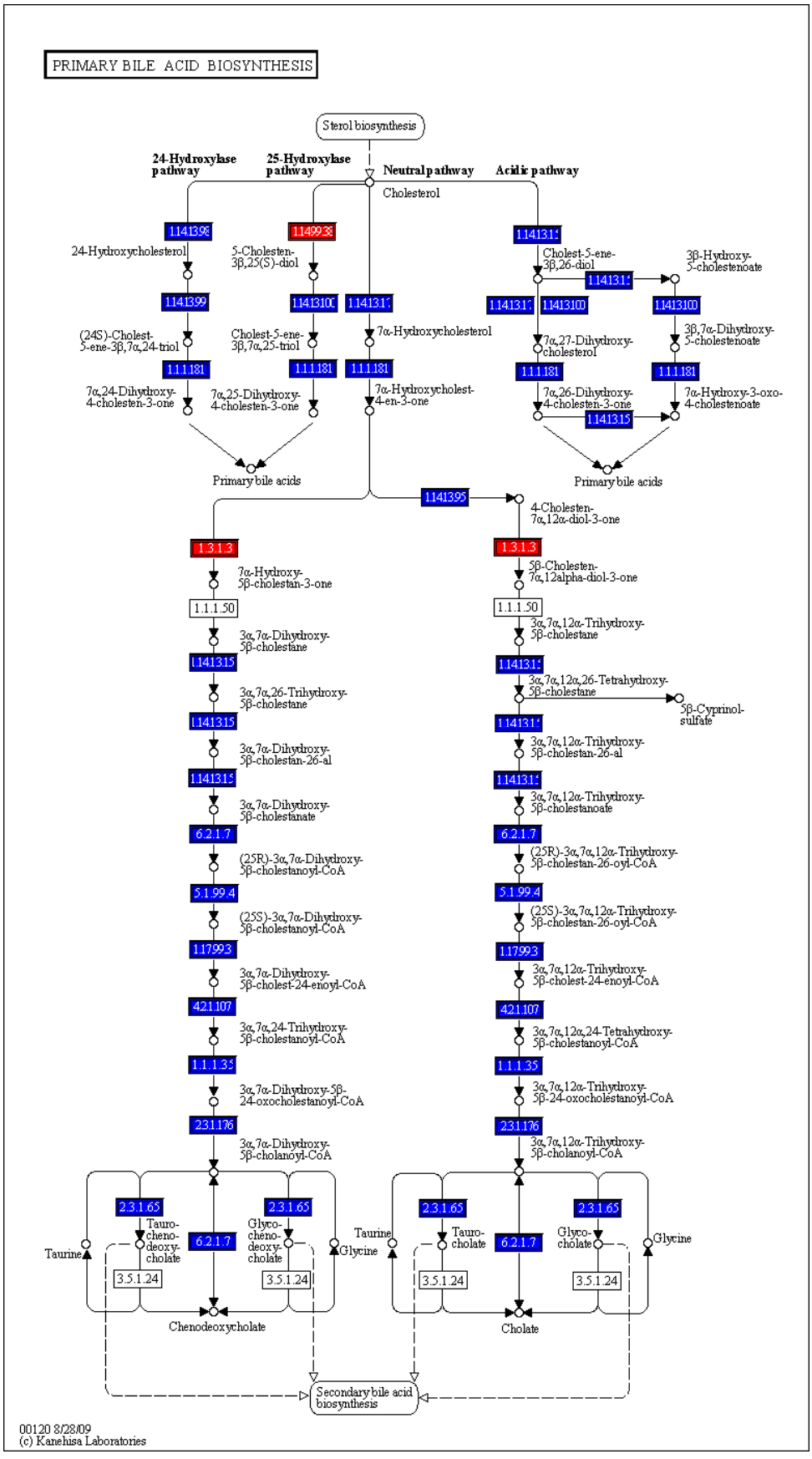

Supplemental Figure 7. (E) Primary bile acid biosynthesis.

F.

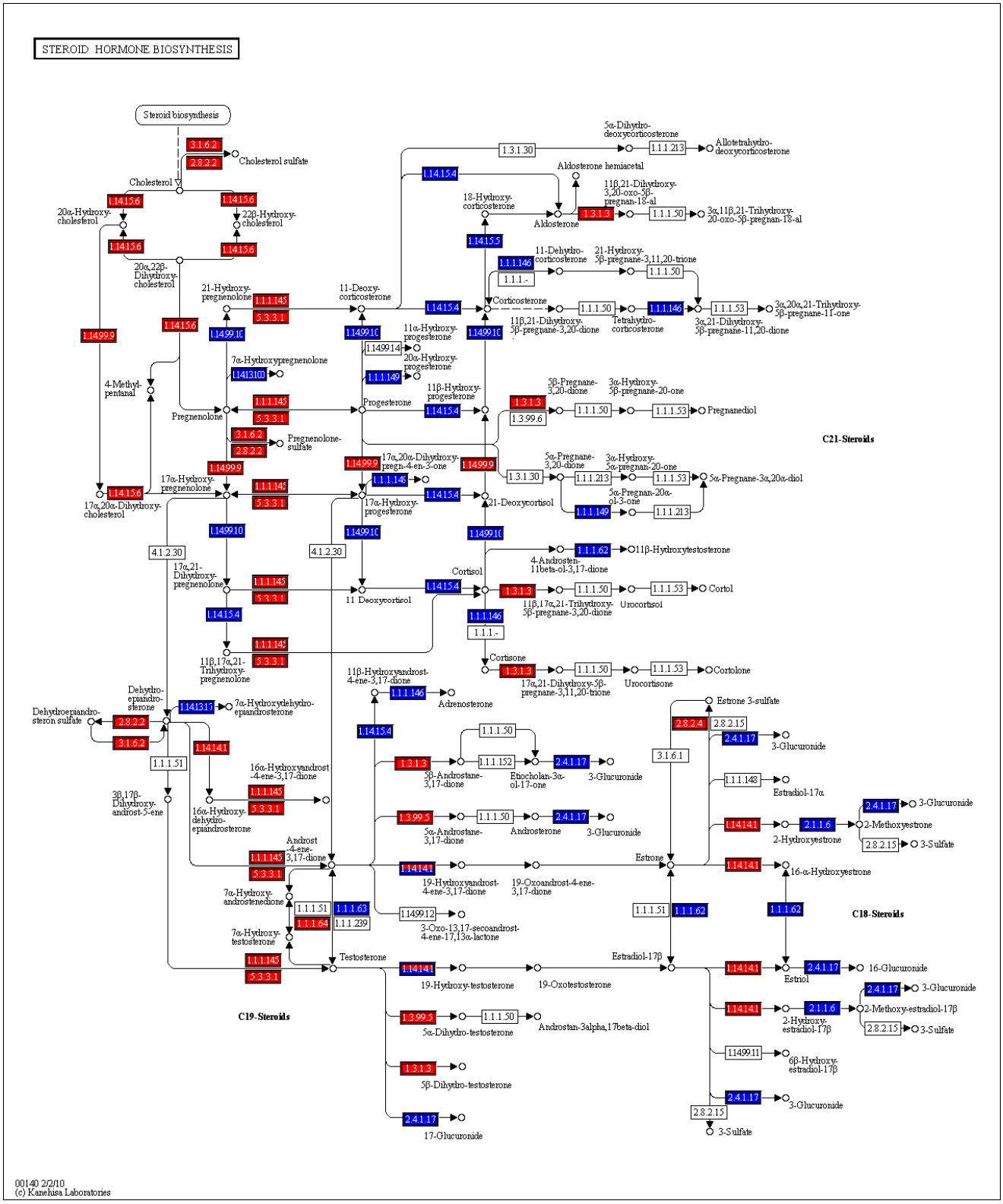

Supplemental Figure 7. (F) Steroid hormone biosynthesis.

	$T_{1/2}$		
	WT	**122KO**	***P* Value**
2.5-month	89.6±22.5 (n=3)	61.7±4.7 (n=3)	*P* >0.05
6-month	130.9±81.6 (n=5)	99.2±18.4 (n=3)	*P* >0.05
P Value	*P* >0.05	*P* >0.05	

$T_{1/2}$: Half time of biliary clearance of ^{99m}Tc-EHIDA; WT: wild type mice, 122KO: *Mir122a*$^{-/-}$ mice.

Supplemental Figure 8. Comparison of half time of biliary clearance of ^{99m}Tc-EHIDA between *Mir122a*$^{-/-}$ and wild type mice. ^{99m}Tc-EHIDA was used in SPECT (Single photon emission computerized tomography) to analyze the biliary clearance. All mice were fasted for 6 hr. The hepatobiliary scintigraphy acquisitions were done on a triple head CZT gamma camera with a built-in CT component (Triumph-SPECT, Gamma Medica) equipped with a high resolution single pinhole collimator (focal length 90.0 mm, aperture diameter 0.5 mm). Before injection, mice were fixed in prone position on the table and anesthetized with 1% isoflurane. The 99mTc-EHIDA dynamic planar imaging with FOV covering the heart, liver and upper abdomen were acquired immediately after tail vein injection of 0.5 mCi/0.15ml radiotracer and obtained at 1 frame per 300 sec for 120 min. The energy window was set at 140 keV ^{99m}Tc peak with a 20% band. All data are expressed as means ±SD and are compared between groups (122KO vs. WT) using the Student t test. *$p < 0.05$.

The biliary clearance seems to be facilitated in *Mir122a*$^{-/-}$ mice, but the difference is not significant, probably due to large variation and small numbers of mice being tested. There is no confirmed cholestasis in *Mir122a*$^{-/-}$ mice.

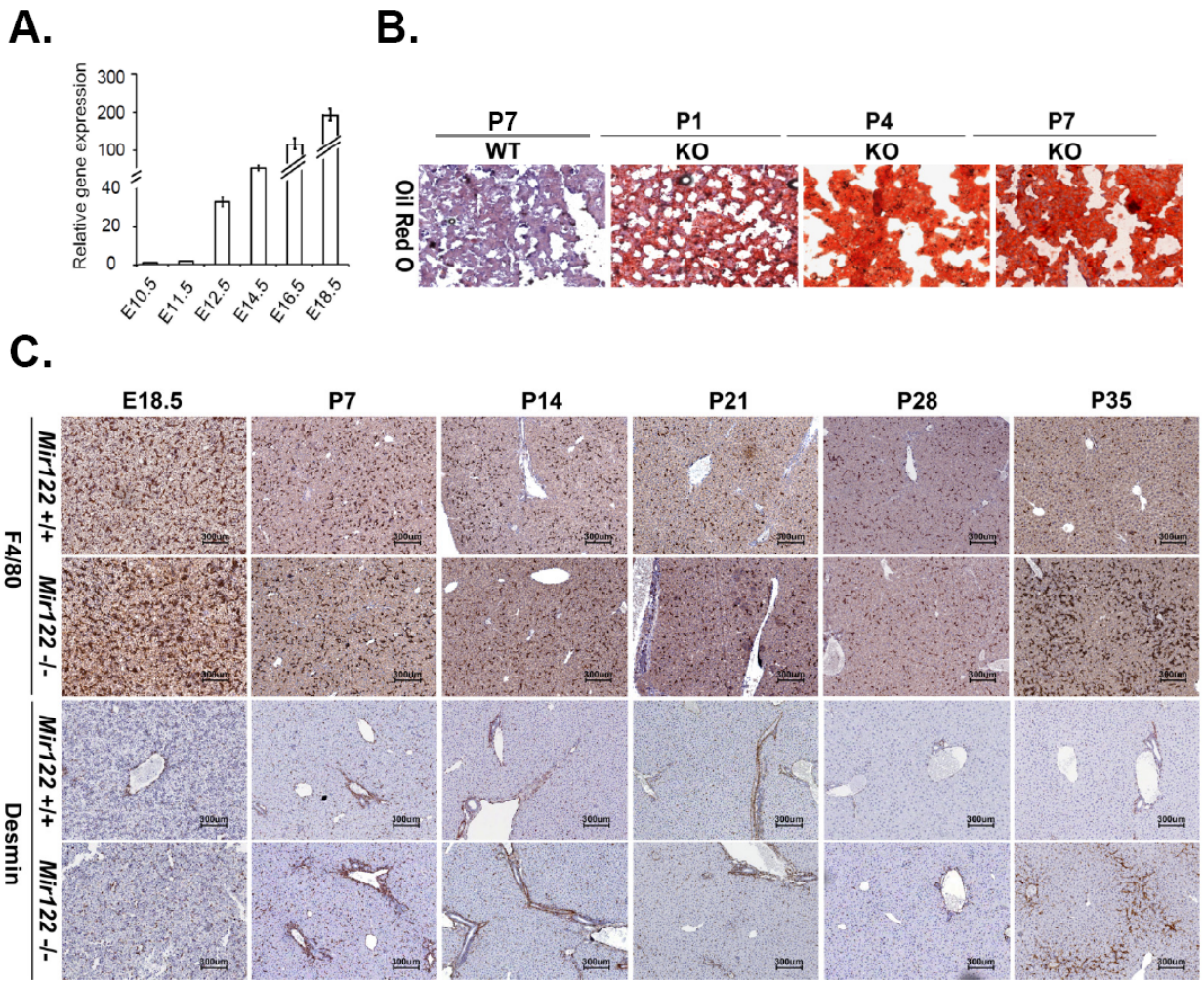

Supplemental Figure 9. The orderly development of steatohepatitis and liver fibrosis was detected in young *Mir122a*$^{-/-}$ mice. **(A)** Expression of *Mir122a* was detected in E12.5 ~ E18.5 fetal livers by qRT-PCR. A low level of *Mir122a* can be detected in the E11.5 fetal livers. **(B)** The hepatic steatosis (Oil Red O) was detected in the new born mice. **(C)** Progressive increase in the number of Kupffer cells (F4/80 antibody) and activation of hepatic stellate cells near the portal regions (anti-Desmin antibody) in *Mir122a*$^{-/-}$ livers became visible at one month of age (P35). The bar on the histological sections represents 100 μm. n=3. E18.5 fetal liver; P1, 4, 7, 14, 21, 28, 35, days after birth. *Mir122a*$^{+/+}$, WT; *Mir122a*$^{-/-}$, 122KO mice

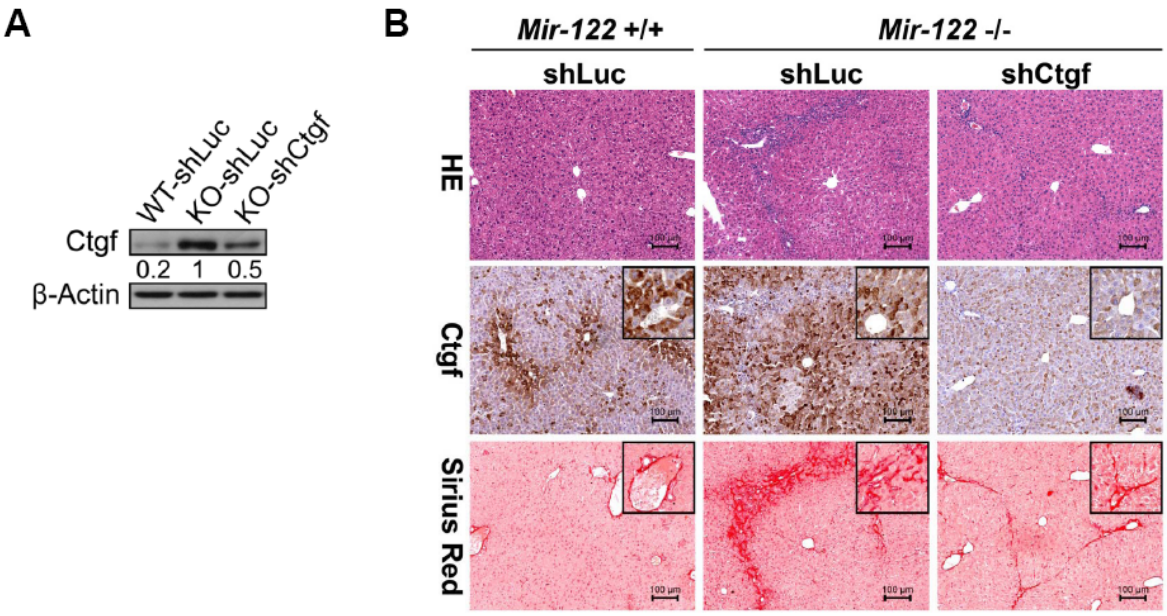

Supplemental Figure 10. shRNA-mediated knockdown of *Ctgf* led to a decrease in hepatic fibrogenesis in *Mir122a*$^{-/-}$ mice. Hydrodynamic injection of shCtgf reduced the expression of Ctgf as shown by western blotting (**A**) and by IHC (**B**). Reduced collagen deposition (Sirius Red staining) was seen in *Mir122a*$^{-/-}$ mice received shCtgf but not in mice received shLuc, which is the control shRNA against Luciferase gene. n=3 mice per group. *Mir122a* $^{+/+}$: wild-type mice; *Mir122a*$^{-/-}$: *mir-122* KO mice.

Supplemental Table 1. Hepatic lipid contents in WT and *Mir122a*$^{-/-}$ mice determined by ^{1}H-NMR

Assignment[a]	Chemical shifts (δ , ppm)	WT (n=5)[b]	*mir-122* KO (n=7)[b]	*P* value
Total cholesterol C-18, C**H**$_3$	0.693-0.664	1.48±0.18	13.78±12.10	0.0362
Total cholesterol C-26, C**H**$_3$/C-27, C**H**$_3$	0.867-0.838	7.43±2.33	63.31±44.47	0.0161
Fatty acyl chain C**H**$_3$(CH$_2$)$_n$	0.885-0.867	12.60±1.51	76.99±61.51	0.0325
Total cholesterol C-21, C**H**$_3$	0.942-0.900	6.50±1.31	50.25±41.71	0.0323
Free cholesterol C-19, C**H**$_3$	1.017-1.000	1.99±0.25	11.76±10.25	0.0453
Esterified cholesterol C-19, C**H**$_3$	1.032-1.017	0.86±0.17	11.89±8.77	0.0158
Multiple cholesterol protons	1.185-1.059	6.55±1.38	63.68±49.59	0.0226
Fatty acyl chain (C**H**$_2$)$_n$	1.412-1.202	311.60±44.61	2371.60±1786.15	0.0225
Multiple cholesterol protons	1.522-1.419	5.73±1.16	31.56±31.12	0.0708
Fatty acyl chain -C**H**$_2$CH$_2$CO	1.666-1.524	32.68±4.40	921.51±1592.95	0.1903
Multiple cholesterol protons	1.904-1.789	2.44±0.20	21.79±18.69	0.0338
Fatty acyl chain -C**H**$_2$CH=	2.151-1.966	170.23±260.17	314.98±208.98	0.3782
Fatty acyl chain -C**H**$_2$CO	2.358-2.213	33.15±4.94	233.32±199.56	0.0379
Fatty acyl chain =CHC**H**$_2$CH=	2.903-2.727	43.69±6.65	194.89±186.75	0.0762
Sphingomyelin and choline N(C**H**$_3$)$_3$	3.402-3.238	23.08±2.57	95.91±81.46	0.0560
Free cholesterol C-3, C**H**	3.579-3.457	6.49±1.20	21.90±16.60	0.0501
Phosphatidylcholine N-C**H**$_2$	3.826-3.693	7.89±0.60	83.33±54.73	0.0108
Glycerophospholipid backbone C-3, C**H**$_2$	4.011-3.839	13.74±1.10	101.70±74.68	0.0207
Triacylglycerol backbone C-1, C**H**$_2$	4.203-4.029	15.16±1.81	108.53±87.56	0.0303
Triacylglycerol backbone C-3, C**H**$_2$	4.386-4.247	13.37±1.66	89.98±95.45	0.0780
Phosphatidylcholine PO-C**H**$_2$	4.444-4.386	2.71±0.39	91.72±97.52	0.0522
Esterified cholesterol C-3, C**H**	4.757-4.701	0.21±0.15	4.08±2.98	0.0138
Glycerolphospholipid backbone C-2, C**H**	5.244-5.147	11.58±1.18	110.53±184.90	0.2065
Triacylglycerol backbone C-2, C**H**	5.284-5.242	4.56±1.45	59.43±36.80	0.0076
Fatty acyl chain -**H**C=C**H**-	5.472-5.284	57.43±7.05	368.24±280.43	0.0263

[a]Assignments of chemical shifts were based on authentic samples or values reported in the literature.

[b]Signal intensities were used for quantitation. Data are shown as mean ± SD.

Supplemental Table 2. Nucleotide sequences of the PCR primers for the qRT-PCR assays

Gene		sequence	Gene		sequence
Acaca	F	GGATTCCACGAAAAGAGC	Mlxipl	F	GCGCTTTGACCAGATG
	R	GCTGTAGCAAAAGTGGAG		R	GGAAGTGCTGAGTTGGC
Acly	F	ATGCGAGTGCAGATCC	Mttp	F	AGGCAATTCGAGACAAAG
	R	AAGGTAGTGCCCAATG		R	ACGTCAAAGCATATCGTTC
Afp	F	TCCAGAAGGAAGAGTGGAC	Nr1h2	F	GTGGTGTCTTCTTGAAGATGG
	R	AGACTAGGAGAAGAGAAATAGTT		R	CACTCTTGGAAGACTCAATGG
B2m	F	GACCCTAGTCTTTCTGGTGC	Nr1h3	F	TGTCCACGAGTGACTGTTTC
	R	TTGCTATTTCTTTCTGCGTGC		R	CTGTTGACTCTCCCTTAATGC
Cd90	F	CCCCAGACAGCGAGAGTCTT	Prom1	F	GCTCGTTTTGGAGCTAC
	R	GCCCCTGAGATTAGGAGGTCTT		R	ATTCTTACAAACCAGAGACTG
Cdh1	F	GGAAATGCACCCCTCCAAT	Pklr	F	AGGAGTCTTCCCCTTG
	R	AATCGGCCAGCATTTTCTGT		R	GCGTTTCAGGATATGGTC
Cpt1a	F	ACTGTAAGTCAAAGCCG	Ppara	F	GCTAATAGGATTCAGACAGTGAC
	R	CAGTGAAAGCCCACTC		R	GATTTAAGAGAGTGCACATAGCC
Cpt2	F	ATGCTGTTCACGATGAC	Pparg	F	GTCCATGAGATCATCTACACG
	R	CTCATTACCTTCAGTTGGG		R	ACTGTCATCTAATTCCAGTGC
Epcam	F	CAGCTGGACACCGGCATT	Scd1	F	TAATTGAACACGCGCTC
	R	TGGACCTGCACCTATAAGACGTT		R	ACACCAGGACCTCAATG
Fasn	F	CCAAACTGAGCCTTTTCTACC	Slc27a5	F	CTTGTTGCGAATGTACGAC
	R	AGAAACTTTCCCAGAAATCTTCC		R	GATACGGATGAAATGAGGTG
Foxa1	F	TGGTCATGTCATGCTGAG	Slco1a1	F	TTCAACTGGCCTGTGC
	R	CACTGGATGAGCCAAG		R	GTGCGTCACCGTAGATG
Foxa2	F	GCCTATTATGAACTCATCCTAAG	Slco1a4	F	CCTGTCACACAGTTGG
	R	GAATGACAGATCACTGTGG		R	CCACCGAGATACAGCC
Gsta2	F	AAACCGTTACTTGCCTG	Sox4	F	CTCGCCTTGGTGATTTC
	R	TCCAAGGGAGGCTTTC		R	CCTAAGCTCAACACAAATGC
Igf2	F	CTTGTCTCTTCCCTACTG	Srebf1	F	CGCACCGTAGAGAAGC
	R	AGGTTTGCGAGCGTTA		R	CTAGAGGTCGGCATGG
Klf6	F	AGATCCTTCTATTTTG	Src	F	AGGAACTAACGAGAACTGT
	R	CTAGACAGGTACTCAA		R	ACCACCACTTCTACCC
Ldlr	F	CAACACTAACACGGAG	Vim	F	TCAAGTGCCTTTACTGCAGTTTTT
	R	AGTACCGAATGTCACGAG		R	TGCTGAGCTTCTTTCTATTCCAAA

F, forward primer; R, reverse primer

Supplemental Table 3. Differentially expressed genes in the livers of 2-month-old male *Mir122a*$^{-/-}$ and WT mice. KO/WT, Expression ratio between *Mir122a*$^{-/-}$ and WT (-1.5≦KO/WT≧1.5).

Probeset	Symbol	KO/WT	Probeset	Symbol	KO/WT	Probeset	Symbol	KO/WT
1448194_a_at	H19	635.58	1439560_x_at	Gm5480	4.96	1450611_at	Orm3	3.32
1419590_at	Cyp2b9	43.71	1460550_at	Mtmr11	4.81	1456873_at	Clic5	3.27
1448152_at	Igf2	34.1	1459740_s_at	Ucp2	4.65	1433883_at	Tpm4	3.26
1433966_x_at	Asns	26.83	1424959_at	Anxa13	4.64	1428055_at	Rian	3.25
1452905_at	Meg3	23.61	1417399_at	Gas6	4.64	1424126_at	Alas1	3.23
1427747_a_at	Lcn2	17.4	1419700_a_at	Prom1	4.64	1451978_at	Loxl1	3.23
1418712_at	Cdc42ep5	13.42	1448416_at	Mgp	4.5	1416046_a_at	Fuca2	3.22
1458442_at	AI132709	12.46	1418449_at	Lad1	4.42	1455162_at	Ttc39a	3.22
1419394_s_at	S100a8	11.28	1425837_a_at	Ccrn4l	4.4	1420378_at	Sftpd	3.2
1449479_at	Cyp2b13	9.87	1452463_x_at	Gm10883	4.34	1455955_s_at	Snx17	3.15
1435196_at	Ntrk2	9.28	1421430_at	Rad51l1	4.29	1456388_at	Atp11a	3.13
1448837_at	Vil1	9.05	1417419_at	Ccnd1	4.28	1444139_at	Ddit4l	3.12
1428223_at	Mfsd2a	8.66	1453435_a_at	Fmo2	4.18	1427963_s_at	Rdh9	3.12
1420438_at	Orm2	8.06	1423611_at	Alpl	4.09	1433916_at	Vamp3	3.11
1417821_at	D17H6S56E-5	7.8	1425120_x_at	Ifi27l2b	4.07	1415919_at	Npdc1	3.1
1441102_at	Prlr	7.62	1424305_at	Igj	4.07	1426302_at	Tmprss4	3.08
1425394_at	BC023105	7.38	1424007_at	Gdf10	3.86	1416953_at	Ctgf	3.07
1433610_at	AA986860	6.92	1436643_x_at	Hamp2	3.85	1460351_at	S100a11	3.01
1424649_a_at	Tspan8	6.78	1451780_at	Blnk	3.79	1418962_at	Necap2	2.97
1433575_at	Sox4	6.73	1416596_at	Slc44a4	3.78	1426519_at	P4ha1	2.96
1460406_at	Pls1	6.65	1430172_a_at	Cyp4f16	3.75	1423607_at	Lum	2.94
1456226_x_at	Ddr1	6.55	1455431_at	Slc5a1	3.69	1448735_at	Cp	2.92
1448182_a_at	Cd24a	6.54	1424477_at	Tmem184a	3.68	1460361_at	5033414D02Rik	2.9
1448595_a_at	Bex1	6.41	1416579_a_at	Epcam	3.63	1433816_at	Mcart1	2.9
1433744_at	Lrtm2	6.21	1436991_x_at	Gsn	3.62	1433924_at	Peg3	2.89
1427178_at	Tmc4	5.91	1423669_at	Col1a1	3.59	1418511_at	Dpt	2.86
1416666_at	Serpine2	5.81	1416108_a_at	Tmed3	3.59	1436890_at	Uap1l1	2.86
1417836_at	Gpx7	5.79	1416114_at	Sparcl1	3.5	1416529_at	Emp1	2.84
1429523_a_at	Slc39a5	5.72	1431146_a_at	Cpne8	3.49	1448393_at	Cldn7	2.83
1427357_at	Cda	5.69	1423933_a_at	1600029D21Rik	3.45	1434418_at	Lass6	2.83
1423484_at	Bicc1	5.68	1416432_at	Pfkfb3	3.44	1438377_x_at	Slc13a3	2.83
1449254_at	Spp1	5.68	1439375_x_at	Aldoa	3.41	1427386_at	Arhgef16	2.81
1427020_at	Scara3	5.62	1423707_at	Tmem50b	3.41	1434089_at	Synpo	2.8
1457030_at	Mirg	5.39	1420911_a_at	Mfge8	3.39	1423630_at	Cygb	2.79

1416646_at	Afp	4.98	1419573_a_at	Lgals1	3.34	1448770_a_at	Atpif1	2.78
1438625_s_at	Cdk16	2.78	1417178_at	Gipc2	2.49	1426750_at	Flnb	2.22
1450717_at	Ang	2.76	1426529_a_at	Tagln2	2.49	1428640_at	Hsf2bp	2.22
1417664_a_at	Ndrg3	2.75	1421917_at	Pdgfra	2.47	1460243_at	Sptlc2	2.22
1428066_at	Ccdc120	2.74	1435067_at	B230208H17Rik	2.46	1449145_a_at	Cav1	2.21
1427883_a_at	Col3a1	2.73	1417409_at	Jun	2.46	1455099_at	Mogat2	2.21
1437056_x_at	Crispld2	2.73	1428306_at	Ddit4	2.44	1434944_at	Dmpk	2.19
1428316_a_at	Fundc2	2.73	1418444_a_at	Gde1	2.43	1424229_at	Dyrk3	2.19
1424131_at	Col6a3	2.72	1427201_at	Mustn1	2.43	1419132_at	Tlr2	2.19
1417116_at	Slc6a8	2.72	1425567_a_at	Anxa5	2.41	1426910_at	Pawr	2.18
1434891_at	Ptgfrn	2.71	1439389_s_at	Myadm	2.38	1452016_at	Alox5ap	2.17
1452649_at	Rtn4	2.7	1435156_at	BC046331	2.36	1425896_a_at	Fbn1	2.17
1416517_at	Pnpla6	2.69	1429570_at	Mlkl	2.36	1428715_at	Gfpt1	2.16
1424962_at	Tm4sf4	2.69	1452227_at	Sel1l3	2.36	1435525_at	Kctd17	2.16
1425764_a_at	Bcat2	2.68	1416535_at	Mcrs1	2.35	1435254_at	Plxnb1	2.16
1423217_a_at	Fam32a	2.67	1425921_a_at	1810055G02Rik	2.33	1426397_at	Tgfbr2	2.16
1454078_a_at	Gal3st1	2.67	1451997_at	Zfp426	2.33	1416096_at	Vipar	2.16
1450850_at	Ezr	2.66	1417231_at	Cldn2	2.32	1416656_at	Clic1	2.15
1433521_at	Ankrd13c	2.64	1448111_at	Ctps2	2.32	1450857_a_at	Col1a2	2.15
1435682_at	Lars2	2.64	1460644_at	Bckdk	2.31	1433796_at	Endod1	2.15
1453572_a_at	Plp2	2.64	1422501_s_at	Idh3a	2.31	1417156_at	Krt19	2.13
1436223_at	Itgb8	2.62	1421375_a_at	S100a6	2.31	1449851_at	Per1	2.13
1436902_x_at	Tmsb10	2.62	1455269_a_at	Coro1a	2.3	1427231_at	Robo1	2.13
1424927_at	Glipr1	2.61	1416164_at	Fbln5	2.3	1419569_a_at	Isg20	2.12
1424208_at	Ptger4	2.59	1417360_at	Mlh1	2.29	1448169_at	Krt18	2.12
1419315_at	Slamf9	2.59	1448211_at	Atp6v0e2	2.28	1435653_at	Abhd2	2.11
1416414_at	Emilin1	2.58	1425702_a_at	Enpp5	2.28	1421025_at	Agpat1	2.11
1448873_at	Ocln	2.58	1434301_at	Fam84b	2.28	1449491_at	Card10	2.11
1437843_s_at	Nupl1	2.56	1439543_at	1110064A23Rik	2.27	1454613_at	Dpysl3	2.11
1416110_at	Slc35a4	2.56	1439451_x_at	Gpr172b	2.27	1422780_at	Pxmp4	2.11
1455065_x_at	Gnpda1	2.55	1416789_at	Idh3g	2.27	1425148_a_at	Snx6	2.11
1415779_s_at	Actg1	2.54	1416868_at	Cdkn2c	2.25	1448380_at	Lgals3bp	2.1
1454902_at	Prkcz	2.54	1422549_at	Arl2	2.24	1448569_at	Mlec	2.1
1428795_at	1110021L09Rik	2.52	1431339_a_at	Efhd2	2.23	1424138_at	Rhbdf1	2.1
1416326_at	Crip1	2.52	1454606_at	4933426M11Rik	2.22	1416950_at	Tnfaip8	2.1
1428484_at	Osbpl3	2.52	1421059_a_at	Alg2	2.22	1448162_at	Vcam1	2.1
1460732_a_at	Ppl	2.52	1424240_at	Arfip2	2.22	1428656_at	Rnasen	2.09
1438650_x_at	Gja1	2.51	1423890_x_at	Atp1b1	2.22	1421843_at	Il1rap	2.08
1425173_s_at	Golph3l	2.5	1428442_at	BC029722	2.22	1433776_at	Lhfp	2.08
1437457_a_at	Mtpn	2.08	1452250_a_at	Col6a2	1.97	1416508_at	Med28	1.9

1429214_at	Adamtsl2	2.07	1451126_at	Maf1	1.97	1456292_a_at	Vim	1.9
1451969_s_at	Parp3	2.07	1418300_a_at	Mknk2	1.97	1417240_at	Zyx	1.9
1451190_a_at	Sbk1	2.07	1448995_at	Pf4	1.97	1452304_a_at	Arhgef5	1.89
1416601_a_at	Rcan1	2.06	1422701_at	Zap70	1.97	1435758_at	B4galt6	1.89
1448301_s_at	Serpinb1a	2.06	1418819_at	Arl8b	1.96	1448323_a_at	Bgn	1.89
1418949_at	Gdf15	2.05	1419883_s_at	Atp6v1b2	1.96	1455032_at	Ccnyl1	1.89
1415972_at	Marcks	2.05	1455144_s_at	AU040829	1.96	1451075_s_at	Ctdsp2	1.89
1421448_at	Ralgapa1	2.05	1424478_at	Bbs2	1.96	1416205_at	Glb1	1.89
1427912_at	Cbr3	2.04	1417176_at	Csnk1e	1.96	1455271_at	Gm13889	1.89
1417837_at	Phlda2	2.04	1435465_at	Kbtbd11	1.96	1426523_a_at	Gnpda2	1.89
1436591_at	Vsig10	2.04	1452046_a_at	Ppp1cc	1.96	1452298_a_at	Myo5b	1.89
1422818_at	Nedd9	2.03	1419493_a_at	Tpd52	1.96	1426570_a_at	Frk	1.88
1449066_a_at	Arhgef7	2.02	1417848_at	Zfp704	1.96	1417133_at	Pmp22	1.88
1448823_at	Cxcl12	2.02	1420965_a_at	Enc1	1.95	1428587_at	Tmem41b	1.88
1433870_at	Prr15l	2.02	1436970_a_at	Pdgfrb	1.95	1429722_at	Zbtb4	1.88
1418099_at	Tnfrsf1b	2.02	1418296_at	Fxyd5	1.94	1419115_at	Alg14	1.87
1450667_a_at	Cs	2.01	1423691_x_at	Krt8	1.94	1434086_at	Gpr107	1.87
1420394_s_at	Gp49a	2.01	1417324_at	Mast2	1.94	1426763_at	Oaz2-ps	1.87
1429396_at	Atg16l2	2	1425264_s_at	Mbp	1.94	1451421_a_at	Rogdi	1.87
1448405_a_at	Eid1	2	1450070_s_at	Pak1	1.94	1415822_at	Scd2	1.87
1424215_at	Fundc1	2	1434656_at	Ralgapb	1.94	1429089_s_at	2900026A02Rik	1.86
1429461_at	Ints2	2	1455656_at	Btla	1.93	1455539_at	Gm9983	1.86
1435452_at	Tmem20	2	1417327_at	Cav2	1.93	1455750_at	Ralgapa2	1.86
1458347_s_at	Tmprss2	2	1423392_at	Clic4	1.93	1418101_a_at	Rtn3	1.86
1436236_x_at	Cotl1	1.99	1417612_at	Ier5	1.93	1450138_a_at	Serpinb6a	1.86
1426314_at	Ednrb	1.99	1420863_at	Dctn4	1.92	1417100_at	Cd320	1.85
1449278_at	Eif2ak3	1.99	1456003_a_at	Slc1a4	1.92	1451206_s_at	Cytip	1.85
1454137_s_at	Hfe2	1.99	1452081_a_at	9130017N09Rik	1.91	1449059_a_at	Oxct1	1.85
1450843_a_at	Serpinh1	1.99	1416455_a_at	Cryab	1.91	1422706_at	Pmepa1	1.85
1455506_at	Slc25a34	1.99	1450350_a_at	Jdp2	1.91	1450918_s_at	Src	1.85
1424562_a_at	Slc25a4	1.99	1429527_a_at	Plscr1	1.91	1450196_s_at	Gys1	1.84
1436729_at	Afap1	1.98	1436339_at	1810058I24Rik	1.9	1448606_at	Lpar1	1.84
1460180_at	Hexb	1.98	1432094_a_at	Ccdc132	1.9	1435548_at	Mrs2	1.84
1416452_at	Oat	1.98	1435223_at	Erlin2	1.9	1428842_a_at	Ngfrap1	1.84
1433529_at	Pamr1	1.98	1427474_s_at	Gstm3	1.9	1428154_s_at	Ppapdc1b	1.84
1437234_x_at	Prmt2	1.98	1453304_s_at	Ly6e	1.9	1449110_at	Rhob	1.84
1426434_at	Tmem43	1.98	1422764_at	Mapre1	1.9	1439965_at	Slc43a2	1.84
1455308_at	Ano6	1.83	1434184_s_at	Map4k4	1.76	1451253_at	Pxk	1.7
1436778_at	Cybb	1.83	1418386_at	N6amt2	1.76	1448204_at	Sav1	1.7
1419505_a_at	Ggps1	1.83	1454691_at	Nrxn1	1.76	1452281_at	Sos2	1.7

1416749_at	Htra1	1.83	1418892_at	Rhoj	1.76	1438289_a_at	Sumo1	1.7
1423584_at	Igfbp7	1.83	1448568_a_at	Slc20a1	1.76	1449363_at	Atf3	1.69
1458299_s_at	Nfkbie	1.83	1416627_at	Spint1	1.76	1416328_a_at	Atp6v0e	1.69
1454941_at	Nmt1	1.83	1416281_at	Wdr45l	1.76	1454636_at	Cbx5	1.69
1448123_s_at	Tgfbi	1.83	1418981_at	Casp12	1.75	1417104_at	Emp3	1.69
1438246_at	Csnk1g1	1.82	1417960_at	Cpeb1	1.75	1429104_at	Limd2	1.69
1434041_at	Appbp2	1.81	1425747_at	Dock5	1.75	1427100_at	Metrn	1.69
1448669_at	Dkk3	1.81	1454983_at	Fam63b	1.75	1450971_at	Gadd45b	1.68
1460594_a_at	Gmppa	1.81	1438603_x_at	Masp1	1.75	1448728_a_at	Nfkbiz	1.68
1427742_a_at	Klf6	1.81	1424754_at	Ms4a7	1.75	1434737_at	Obfc1	1.68
1439364_a_at	Mmp2	1.81	1449368_at	Dcn	1.74	1436937_at	Rbms3	1.68
1416687_at	Plod2	1.81	1426648_at	Mapkapk2	1.74	1431744_a_at	Smap1	1.68
1416230_at	Rfk	1.81	1452067_at	Naaa	1.74	1455513_at	Taf1	1.68
1416009_at	Tspan3	1.81	1448392_at	Sparc	1.74	1423824_at	Wls	1.68
1452217_at	Ahnak	1.8	1455566_s_at	Spats2l	1.74	1420008_s_at	Wwc1	1.68
1448901_at	Cpxm1	1.8	1422751_at	Tle1	1.74	1434961_at	Asb1	1.67
1424422_s_at	Flad1	1.8	1430538_at	2210013O21Rik	1.73	1439902_at	C5ar1	1.67
1424351_at	Wfdc2	1.8	1460218_at	Cd52	1.73	1449385_at	Hsd17b6	1.67
1452719_at	Zdhhc24	1.8	1452359_at	Rell1	1.73	1437494_at	Mapkapk3	1.67
1437087_at	2210408K08Rik	1.79	1454890_at	Amot	1.72	1455229_x_at	Pgs1	1.67
1436041_at	LOC100046086	1.79	1429891_at	Capsl	1.72	1426347_at	2010321M09Rik	1.66
1426728_x_at	Ptdss2	1.79	1417394_at	Klf4	1.72	1420820_at	2900073G15Rik	1.66
1435517_x_at	Ralb	1.79	1437165_a_at	Pcolce	1.72	1456307_s_at	Adcy7	1.66
1447621_s_at	Tmem173	1.79	1434592_at	Slc16a10	1.72	1451681_at	BC089597	1.66
1440890_a_at	Zfp809	1.79	1417447_at	Tcf21	1.72	1419004_s_at	Bcl2a1a	1.66
1428373_at	Ip6k2	1.78	1424829_at	A830007P12Rik	1.71	1420804_s_at	Clec4d	1.66
1431056_a_at	Lpl	1.78	1427239_at	Ift122	1.71	1428861_at	Filip1l	1.66
1423989_at	Tecpr1	1.78	1416590_a_at	Rab34	1.71	1448396_at	Tmem131	1.66
1452599_s_at	AI413582	1.77	1434153_at	Shb	1.71	1441811_x_at	Tmem176a	1.66
1448682_at	Dynll1	1.77	1422631_at	Ahr	1.7	1423870_at	Aida	1.65
1427537_at	Eppk1	1.77	1435661_at	Als2cr4	1.7	1434038_at	Dnajc13	1.65
1418301_at	Irf6	1.77	1419350_at	Hook2	1.7	1455793_at	Fam149a	1.65
1420477_at	Nap1l1	1.77	1435514_at	Lztfl1	1.7	1436243_at	Frmd5	1.65
1460717_at	Tspyl1	1.77	1451575_a_at	Nudt3	1.7	1425942_a_at	Gpm6b	1.65
1428245_at	G6pc3	1.76	1426319_at	Pdgfd	1.7	1437716_x_at	Kif22	1.65
1460419_a_at	Prkcb	1.65	1449020_at	Plscr3	1.61	1425332_at	Zfp106	1.57
1451227_a_at	Slc10a3	1.65	1417466_at	Rgs5	1.61	1422013_at	Clec4a2	1.56
1426599_a_at	Slc2a1	1.65	1415874_at	Spry1	1.61	1415702_a_at	Ctbp1	1.56
1417635_at	Spa17	1.65	1434444_s_at	Anapc1	1.6	1443820_x_at	Elovl1	1.56
1419655_at	Tle3	1.65	1428549_at	Ccdc3	1.6	1427927_at	Hscb	1.56

1417510_at	Vps4a	1.65	1427301_at	Cd48	1.6	1421209_s_at	Ikbkg	1.56
1453355_at	Wnk2	1.65	1424113_at	Lamb1-1	1.6	1424438_a_at	Leprot	1.56
1426548_a_at	Atpbd4	1.64	1421820_a_at	Nf2	1.6	1422936_at	Mas1	1.56
1426710_at	Calm3	1.64	1451599_at	Sesn2	1.6	1456531_x_at	Prpf19	1.56
1422439_a_at	Cdk4	1.64	1435802_at	Zbtb45	1.6	1460363_at	Tnrc6c	1.56
1433926_at	Dync1li2	1.64	1436204_at	1110059G02Rik	1.59	1428945_at	Uba6	1.56
1418049_at	Ltbp3	1.64	1459962_at	4930523C07Rik	1.59	1417818_at	Wwtr1	1.56
1436996_x_at	Lyz1	1.64	1424307_at	Arhgap1	1.59	1432445_at	2310016G11Rik	1.55
1449498_at	Marco	1.64	1452850_s_at	Brms1l	1.59	1435959_at	Arhgap15	1.55
1421622_a_at	Rapgef4	1.64	1435910_at	Fads3	1.59	1419605_at	Clec10a	1.55
1452134_at	Tmem175	1.64	1438562_a_at	Ptpn2	1.59	1416514_a_at	Fscn1	1.55
1436669_at	1700019G17Rik	1.63	1424394_at	Selm	1.59	1416554_at	Pdlim1	1.55
1421187_at	Ccr2	1.63	1427889_at	Spna2	1.59	1419279_at	Pip4k2a	1.55
1428196_a_at	Fam82a2	1.63	1418744_s_at	Tesc	1.59	1455422_x_at	Sept4	1.55
1423147_at	Mat1a	1.63	1452745_at	Trappc9	1.59	1455732_at	1700025G04Rik	1.54
1453419_at	Mras	1.63	1420682_at	Chrnb1	1.58	1428671_at	2200002D01Rik	1.54
1439617_s_at	Pck1	1.63	1435188_at	Gm129	1.58	1435751_at	Abcc9	1.54
1428623_at	Plxna1	1.63	1419193_a_at	Gmfg	1.58	1428103_at	Adam10	1.54
1437832_x_at	Wars	1.63	1417044_at	Lcmt1	1.58	1422415_at	Ang2	1.54
1419759_at	Abcb1a	1.62	1416808_at	Nid1	1.58	1448261_at	Cdh1	1.54
1437466_at	Alcam	1.62	1437724_x_at	Pitpnm1	1.58	1449195_s_at	Cxcl16	1.54
1449870_a_at	Atp6v0a2	1.62	1422603_at	Rnase4	1.58	1448557_at	Fam13c	1.54
1436921_at	Atp7a	1.62	1450377_at	Thbs1	1.58	1455002_at	Ptp4a1	1.54
1455688_at	Ddr2	1.62	1452633_s_at	Aak1	1.57	1459897_a_at	Sbsn	1.54
1452005_at	Dlat	1.62	1451016_at	Ifrd2	1.57	1449579_at	Sh3yl1	1.54
1428135_a_at	Eef1d	1.62	1423960_at	Lpcat3	1.57	1422629_s_at	Shroom3	1.54
1428101_at	Rnf38	1.62	1424850_at	Map3k1	1.57	1417881_at	Slc39a3	1.54
1416153_at	Srp54a	1.62	1437462_x_at	Mmp15	1.57	1429556_at	Tead1	1.54
1452150_at	AU040320	1.61	1417349_at	Pldn	1.57	1453303_at	4833417J20Rik	1.53
1425911_a_at	Fgfr1	1.61	1423355_at	Snap29	1.57	1451002_at	Aco2	1.53
1424686_at	Heatr6	1.61	1427689_a_at	Tnip1	1.57	1448484_at	Amd1	1.53
1451629_at	Lbh	1.61	1435549_at	Trpm4	1.57	1434745_at	Ccnd2	1.53
1418231_at	Lims1	1.61	1456043_at	Usp22	1.57	1424376_at	Cdc42ep1	1.53
1426955_at	Col18a1	1.53	1435740_at	Gm10397	1.5	1423831_at	Prkag2	-1.54
1449252_at	Fam110c	1.53	1419197_x_at	Hamp	1.5	1460704_at	Rfng	-1.54
1421323_a_at	G3bp2	1.53	1419459_a_at	Magt1	1.5	1460323_at	Tars	-1.54
1424994_at	Glyctk	1.53	1429582_at	Nacc2	1.5	1455278_at	Wdr37	-1.54
1426306_a_at	Maged2	1.53	1429507_at	Nkd1	1.5	1447550_at	Gm8350	-1.55
1422671_s_at	Naalad2	1.53	1428493_at	Sipa1l3	1.5	1417932_at	Il18	-1.55
1421266_s_at	Nfkbib	1.53	1417392_a_at	Slc7a7	1.5	1436120_at	Setdb2	-1.55

1426726_at	Ppp1r10	1.53	1430170_at	Bbs10	-1.5	1453065_at	Aldh5a1	-1.56
1416360_at	Snx18	1.53	1442073_at	Inpp1	-1.5	1424583_at	Farp2	-1.56
1421891_at	St3gal2	1.53	1452291_at	Arap2	-1.51	1431078_at	Fbxo3	-1.56
1425536_at	Stx3	1.53	1458295_at	BC038331	-1.51	1418885_a_at	Idh3b	-1.56
1418004_a_at	Tmem176b	1.53	1424436_at	Gart	-1.51	1449157_at	Nr2c1	-1.56
1420295_x_at	Clcn5	1.52	1460689_at	Pppde2	-1.51	1421204_a_at	Nudt16	-1.56
1417477_at	Gm16515	1.52	1422656_at	Rasl2-9-ps	-1.51	1438933_x_at	Rasgrp2	-1.56
1455277_at	Hhip	1.52	1420919_at	Sgk3	-1.51	1433645_at	Slc44a1	-1.56
1448452_at	Irf8	1.52	1433933_s_at	Slco2b1	-1.51	1436138_at	Ttc19	-1.56
1427060_at	Mapk3	1.52	1443652_x_at	Spred1	-1.51	1416607_at	4931406C07Rik	-1.57
1416331_a_at	Nfe2l1	1.52	1417174_at	Tmem218	-1.51	1428516_a_at	Alkbh7	-1.57
1424214_at	Parm1	1.52	1455281_at	Wdr33	-1.51	1449839_at	Casp3	-1.57
1416400_at	Pycrl	1.52	1443901_at	C2cd2	-1.52	1417015_at	Rassf3	-1.57
1416882_at	Rgs10	1.52	1435380_at	Cox10	-1.52	1436167_at	Shf	-1.57
1434918_at	Sox6	1.52	1426440_at	Dhrs7	-1.52	1418412_at	Tpd52l1	-1.57
1435568_at	Ttc37	1.52	1437301_a_at	Dvl1	-1.52	1431879_at	9030417H13Rik	-1.58
1448100_at	4833439L19Rik	1.51	1445898_at	Ggcx	-1.52	1433759_at	Dpy19l1	-1.58
1418128_at	Adcy6	1.51	1451552_at	Lipt1	-1.52	1437829_s_at	Eef2k	-1.58
1454169_a_at	Epsti1	1.51	1418034_at	Mrps9	-1.52	1419228_at	Elac1	-1.58
1416199_at	Kifc3	1.51	1424488_a_at	Ppa2	-1.52	1451058_at	Mcts2	-1.58
1455487_at	Mfsd11	1.51	1424792_at	Rpp40	-1.52	1419400_at	Mttp	-1.58
1428609_at	Myl12b	1.51	1449125_at	Tnfaip8l1	-1.52	1458408_at	Samd8	-1.58
1418831_at	Pkp3	1.51	1441842_s_at	Zfp707	-1.52	1453208_at	2700089E24Rik	-1.59
1416260_a_at	Snx1	1.51	1447753_at	Cdc37l1	-1.53	1451723_at	Cnot6l	-1.59
1426248_at	Stk24	1.51	1450484_a_at	Cmpk2	-1.53	1455163_at	Guf1	-1.59
1441945_s_at	Abhd14a	1.5	1417264_at	Coq5	-1.53	1418927_a_at	Habp4	-1.59
1450008_a_at	Ctnnb1	1.5	1451462_a_at	Ifnar2	-1.53	1420846_at	Mrps2	-1.59
1426880_at	Etl4	1.5	1451609_at	Tspan33	-1.53	1416090_at	Pdhb	-1.59
1443838_x_at	Fads2	1.5	1438006_at	4933439F18Rik	-1.54	1451956_a_at	Sigmar1	-1.59
1423829_at	Fam49b	1.5	1455575_at	Eif4ebp2	-1.54	1437345_a_at	Bscl2	-1.6
1421263_at	Gabra3	1.5	1430555_s_at	Lrig3	-1.54	1451141_at	Mettl8	-1.6
1451331_at	Ppp1r1b	-1.6	1417434_at	Gpd2	-1.66	1451518_at	Zfp709	-1.74
1448800_at	Rtn4ip1	-1.6	1457363_at	LOC654469	-1.66	1432562_at	1110006G14Rik	-1.75
1417421_at	S100a1	-1.6	1419173_at	Acy1	-1.67	1418943_at	B230120H23Rik	-1.75
1418490_at	Sdsl	-1.6	1417704_a_at	Arhgap6	-1.67	1433646_at	Mrps27	-1.75
1436867_at	Srl	-1.6	1419697_at	Cxcl11	-1.67	1421014_a_at	Clybl	-1.76
1416345_at	Timm8a1	-1.6	1453796_a_at	Ergic2	-1.67	1454867_at	Mn1	-1.76
1452626_a_at	1810014F10Rik	-1.61	1428767_at	Gsdmd	-1.67	1450852_s_at	F2r	-1.77
1443873_at	4933403F05Rik	-1.61	1426245_s_at	Mapre2	-1.67	1450869_at	Fgf1	-1.77
1419261_at	Acad8	-1.61	1435036_at	Aspg	-1.68	1437067_at	Phtf2	-1.77

1452532_x_at	Ceacam1	-1.61	1428490_at	C1galt1	-1.68	1430077_at	Sfrs11	-1.77
1436532_at	Dclk3	-1.61	1430814_at	Cyp2d40	-1.68	1423447_at	Clpx	-1.79
1437858_at	Dpy19l3	-1.61	1451426_at	Dhx58	-1.68	1429188_at	Cox11	-1.79
1417080_a_at	Ecsit	-1.61	1452353_at	Gpr155	-1.68	1458436_at	Auh	-1.8
1416555_at	Ei24	-1.61	1430287_s_at	Hemk1	-1.68	1425701_a_at	Rgs3	-1.8
1424698_s_at	Gca	-1.61	1419362_at	Mrpl35	-1.68	1459813_at	1700012D01Rik	-1.82
1453678_at	Mbd1	-1.61	1453255_at	Slc43a1	-1.68	1449052_a_at	Dnmt3b	-1.82
1448825_at	Pdk2	-1.61	1418658_at	Fam82b	-1.69	1455037_at	Plxna2	-1.82
1459838_s_at	Btbd11	-1.62	1460231_at	Irf5	-1.69	1424022_at	Osgin1	-1.83
1437339_s_at	Pcsk5	-1.62	1438640_x_at	Pgk1	-1.69	1449371_at	Hars2	-1.84
1452917_at	Rfc5	-1.62	1436058_at	Rsad2	-1.69	1418835_at	Phlda1	-1.84
1448930_at	3010026O09Rik	-1.63	1436164_at	Slc30a1	-1.69	1429206_at	Rhobtb1	-1.84
1446368_at	9130221J18Rik	-1.63	1452207_at	Cited2	-1.7	1422852_at	Cib2	-1.85
1438198_at	Bri3bp	-1.63	1428556_at	Pigy	-1.7	1418474_at	Fam158a	-1.85
1455118_at	D9Ertd402e	-1.63	1431722_a_at	Afmid	-1.71	1448021_at	Fam46c	-1.85
1432249_a_at	Ercc8	-1.63	1421756_a_at	Gpr19	-1.71	1459860_x_at	Trim2	-1.85
1451512_s_at	Hibch	-1.63	1428507_at	Hdhd2	-1.71	1431694_a_at	Ctnnbip1	-1.86
1435043_at	Plcb1	-1.63	1431591_s_at	Isg15	-1.71	1424352_at	Cyp4a12a	-1.86
1451277_at	Zadh2	-1.63	1429863_at	Lonrf3	-1.71	1418267_at	Mst1	-1.86
1434232_a_at	2610030H06Rik	-1.64	1429216_at	Paqr3	-1.71	1421309_at	Mgmt	-1.87
1428897_at	2610029I01Rik	-1.65	1420515_a_at	Pglyrp2	-1.71	1424760_a_at	Smyd2	-1.87
1451114_at	Cmtm6	-1.65	1437932_a_at	Cldn1	-1.72	1425117_at	Aspdh	-1.88
1448535_at	Elp4	-1.65	1460591_at	Esr1	-1.72	1427573_at	Chic1	-1.88
1423972_at	Etfa	-1.65	1449062_at	Khk	-1.72	1436959_x_at	Nelf	-1.88
1451354_at	Foxred1	-1.65	1431032_at	Agl	-1.73	1450627_at	Ank	-1.89
1449348_at	Mpp6	-1.65	1449576_at	Eif1ax	-1.73	1426669_at	Cpped1	-1.89
1429749_at	Sfmbt1	-1.65	1458678_at	Ndufab1	-1.73	1436070_at	Glo1	-1.89
1416479_a_at	Tmem14c	-1.65	1416940_at	Ppif	-1.74	1431805_a_at	Rhpn2	-1.89
1453985_at	0610007P08Rik	-1.66	1443962_at	Tfdp2	-1.74	1431422_a_at	Dusp14	-1.9
1437424_at	Syde2	-1.9	1449155_at	Polr3g	-2.21	1437424_at	Syde2	-1.9
1436109_at	AI317395	-1.91	1422815_at	C9	-2.24	1436109_at	AI317395	-1.91
1443822_s_at	Cisd1	-1.91	1453011_at	Bdh2	-2.25	1443822_s_at	Cisd1	-1.91
1456767_at	Lrfn3	-1.91	1460059_at	Upp2	-2.25	1456767_at	Lrfn3	-1.91
1418997_at	Lyrm5	-1.91	1424692_at	2810055F11Rik	-2.28	1418997_at	Lyrm5	-1.91
1420654_a_at	Gbe1	-1.92	1435245_at	Gls2	-2.28	1420654_a_at	Gbe1	-1.92
1422399_a_at	Rab23	-1.93	1418311_at	Fn3k	-2.29	1422399_a_at	Rab23	-1.93
1445787_at	Ccdc162	-1.94	1434692_at	1110034B05Rik	-2.31	1445787_at	Ccdc162	-1.94
1442191_at	5033411D12Rik	-1.95	1419510_at	Es22	-2.32	1442191_at	5033411D12Rik	-1.95
1448350_at	Asl	-1.95	1418645_at	Hal	-2.34	1448350_at	Asl	-1.95
1450033_a_at	Stat1	-1.95	1427213_at	Pfkfb1	-2.34	1450033_a_at	Stat1	-1.95

1440688_at	Arhgap26	-1.96	1452975_at	Agxt2l1	-2.36	1440688_at	Arhgap26	-1.96
1417869_s_at	Ctsz	-1.97	1460318_at	Csrp3	-2.36	1417869_s_at	Ctsz	-1.97
1456181_at	Wdr91	-1.98	1425778_at	Ido2	-2.37	1456181_at	Wdr91	-1.98
1449038_at	Hsd11b1	-1.99	1439459_x_at	Acly	-2.38	1449038_at	Hsd11b1	-1.99
1452864_at	Med12l	-2.03	1429503_at	Fam69a	-2.38	1452864_at	Med12l	-2.03
1428859_at	Paox	-2.03	1438055_at	Rarres1	-2.38	1428859_at	Paox	-2.03
1457027_at	Dhtkd1	-2.05	1429399_at	Rnf125	-2.39	1457027_at	Dhtkd1	-2.05
1419670_at	Ftcd	-2.07	1449375_at	Ces6	-2.4	1419670_at	Ftcd	-2.07
1446769_at	Ttc39c	-2.07	1453187_at	Ociad2	-2.4	1446769_at	Ttc39c	-2.07
1441110_at	Lrit1	-2.08	1425778_at	Ido2	-2.37	1451615_at	Ces8	-2.96
1428091_at	Klhl7	-2.09	1439459_x_at	Acly	-2.38	1422478_a_at	Acss2	-3.02
1459141_at	1810008I18Rik	-2.1	1429503_at	Fam69a	-2.38	1429642_at	Anubl1	-3.1
1424921_at	Bst2	-2.1	1438055_at	Rarres1	-2.38	1424716_at	Retsat	-3.11
1434410_at	Crybg3	-2.1	1429399_at	Rnf125	-2.39	1451418_a_at	Spsb4	-3.13
1450237_at	Dnase2b	-2.11	1449375_at	Ces6	-2.4	1453500_at	Cyp2u1	-3.14
1418837_at	Qprt	-2.12	1453187_at	Ociad2	-2.4	1416795_at	Cryl1	-3.32
1430319_at	4833411C07Rik	-2.13	1420603_s_at	Raet1a	-2.44	1423186_at	Tiam2	-3.56
1449945_at	Ppargc1b	-2.17	1422735_at	Foxq1	-2.45	1427052_at	Acacb	-3.57
1420362_a_at	Bik	-2.19	1416049_at	Gldc	-2.46	1453752_at	Rpl17	-3.62
1437492_at	Mkx	-2.19	1421987_at	Papss2	-2.48	1416855_at	Gas1	-3.73
1432282_a_at	Tlcd2	-2.2	1418519_at	Aadat	-2.5	1421183_at	Tex12	-3.82
1433733_a_at	Cry1	-2.21	1427370_at	Amdhd1	-2.51	1417765_a_at	Amy1	-3.85
1449155_at	Polr3g	-2.21	1438676_at	Mpa2l	-2.55	1456074_at	Sdr9c7	-3.92
1422815_at	C9	-2.24	1418857_at	Slc13a2	-2.55	1436931_at	Rfx4	-4.3
1453011_at	Bdh2	-2.25	1435836_at	Pdk1	-2.56	1421830_at	Ak3	-4.76
1460059_at	Upp2	-2.25	1435084_at	C730049O14Rik	-2.57	1418780_at	Cyp39a1	-4.82
1424692_at	2810055F11Rik	-2.28	1426450_at	Plcl2	-2.57	1453220_at	Fam55b	-5.22
1435245_at	Gls2	-2.28	1444138_at	Cyp2r1	-2.6	1421092_at	Serpina12	-5.32
1418311_at	Fn3k	-2.29	1442612_at	C730036E19Rik	-2.65	1455383_at	Fam47e	-5.65
1434692_at	1110034B05Rik	-2.31	1457915_at	4833442J19Rik	-2.66	1450917_at	Myom2	-5.8
1419510_at	Es22	-2.32	1454159_a_at	Igfbp2	-2.66	1434449_at	Aqp4	-6.54
1418645_at	Hal	-2.34	1448898_at	Ccl9	-2.78	1455991_at	Ccbl2	-7.41
1427213_at	Pfkfb1	-2.34	1437250_at	Mreg	-2.78	1420722_at	Elovl3	-9.89
1452975_at	Agxt2l1	-2.36	1417828_at	Aqp8	-2.92	1423397_at	Ugt2b38	-22.52
1460318_at	Csrp3	-2.36	1457619_at	BC015286	-2.92			

Supplementary Table 4. GSEA analysis of 2-month-old male *mir-122*$^{-/-}$ and wild-type mice. The pathways are ranked by Norminal Enrichment Score (NES).

Pathway ID	Map Name	Norminal enrichment score (NES)	Nominal p-value	FDR q-val	Enriched in phenotype	List size	Leading edge gene count	Leading egde Gene Symbol
*CGU00001	Liver fibrosis	2.3036	0.0000	0.0000	KO	23	15	Ddr1, Col1a2, Cygb, Ctgf, Klf6, Col1a1, Loxl1, Col3a1, Col6a3, Pdgfra, Pdgfd, Timp1, Pdgfrb, Col6a2, Vcam1
MMU04510	Focal adhesion	2.2310	0.0000	0.0000	KO	194	92	Itgb8, Col1a2, Spp1, Ccnd1, Col1a1, Cav1, Itga6, Col3a1, Thbs1, Col5a2, Pik3r5, Col6a1, Hgf, Pak1, Lama2, Pdgfra, Pdgfd, Lamc3, Pdgfrb, Prkca, Itga8, Actg1, Src, Col6a2, Parvb, Mapk3, Vwf, Zyx, Jun, Col4a2, Lamb2, Thbs2, Lamb1-1, Col4a1, Vegfc, Comp, Rac2, Pak3, Myl2, Bcl2, Pdgfa, Flna, Bad, Vasp, Cav2, Myl12b, Itga4, Myl9, Ppp1cc, Lama1, Pak6, Pik3r3, Shc4, Pdgfc, Sos2, Ccnd2, Fyn, Ctnnb1, Pik3cd, Met, 2900073G15Rik, Itgb3, Prkcb, Rock2, Birc2, Pik3cg, Vav1, Pdgfb, Myl10, Pak2, Myl7, Lama5, Diap1, Rap1b, Vav3, Crkl, Parvg, Dock1, Lama4, Pik3ca, Itga2, Col4a4, Rac3, Igf1r, Ilk, Flt1, Mapk1, Erbb2, Gsk3b, Lamc1, Itgb4, Mylpf
MMU04512	ECM-receptor interaction	2.2023	0.0000	0.0003	KO	81	22	Itgb8, Col1a2, Spp1, Col1a1, Itga6, Col3a1, Thbs1, Col5a2, Col6a1, Lama2, Cd44, Lamc3, Itga8, Col6a2, Vwf, Col4a2, Lamb2, Thbs2, Lamb1-1, Col4a1, Npnt, Comp
MMU05150	Staphylococcus aureus infection	2.1141	0.0000	0.0002	KO	47	21	Ighg, H2-Ab1, H2-Eb1, H2-Aa, Itgb2, H2-Oa, Masp1, Fcgr3, Fpr2, Icam1, C3ar1, Selplg, Fpr1, Itgam, H2-Ob, C5ar1, H2-DMb2, Fcgr1, Cfd, C1qc, H2-DMa
MMU05140	Leishmaniasis	2.0904	0.0000	0.0004	KO	65	29	Ighg, H2-Ab1, H2-Eb1, H2-Aa, Cyba, Tgfb3, Tgfb2, Itgb2, H2-Oa, Tlr2, Mapk3, Jun, Fcgr3, Ncf1, Mapk13, Itgam, Marcksl1, Itga4, Tlr4, H2-Ob, H2-DMb2, Ncf4, Fcgr1, Nfkbia, H2-DMa, Prkcb, Irak4, Jak1, Nfkbib
MMU04514	Cell adhesion molecules (CAMs)	2.0583	0.0000	0.0006	KO	130	43	Cldn7, Itgb8, Cd34, Itga6, H2-Ab1, H2-Eb1, Ocln, H2-Aa, Cldn8, Itgb2, H2-Oa, Itga8, Sell, Cldn2, Vcam1, Jam2, Cd2, Pvrl1, Cldn6, Icam1, Selplg, Cldn23, Cd28, Itgam, Alcam, Cd99, Itga4, Pvrl2, Cd40, H2-Ob, Cd86, Cntnap1, H2-DMb2, Cd276, Nlgn1, Sdc1, Nrxn2, Icam2, H2-DMa, Cdh1, Negr1, Glg1, Pecam1
MMU04145	Phagosome	1.9737	0.0000	0.0033	KO	147	43	Sftpd, Vamp3, Coro1a, Cd14, Cybb, Atp6v0e2, Ighg, H2-Ab1, Thbs1, H2-Eb1, Cd209a, H2-Aa, Cyba, Itgb2, H2-Oa, Tlr2, Actg1, Marco, Tubb2b, Thbs2, Fcgr3, Ncf1, Comp, Atp6v0e, Dync1li2, Atp6v0a2, Atp6v1b2, Cd209d, Itgam, Tuba1a, Mrc2, Tlr4, H2-Ob, Atp6v0d2, Mpo, H2-DMb2, Ncf4, Rab5c, Fcgr1, Atp6v1g2, H2-DMa, Itgb3, Ctss
MMU05146	Amoebiasis	1.9417	0.0000	0.0041	KO	107	31	Serpinb1a, Col1a2, Serpinb6b, Cd14, Col1a1, Col3a1, Ighg, Col5a2, Pik3r5, Gna14, Lama2, Tgfb3, Tgfb2, Lamc3, Itgb2, Tlr2, Prkca, Arg2, Serpinb6a, Col4a2, Lamb2, Lamb1-1, Col4a1, Itgam, Lama1, Pik3r3, Tlr4, Gna15, Il1r2, Rab5c, Pik3cd
MMU05310	Asthma	1.9043	0.0016	0.0054	KO	25	12	Ighg, H2-Ab1, H2-Eb1, H2-Aa, H2-Oa, Prg2, Cd40, H2-Ob, H2-DMb2, H2-DMa, Il5, Fcer1g
MMU04810	Regulation of actin cytoskeleton	1.8791	0.0000	0.0070	KO	207	77	Itgb8, Gsn, Cd14, Itga6, Fgf21, Pik3r5, Pak1, Pdgfra, Pdgfd, Fgfr1, Pip4k2a, Ezr, Was, Itgax, Itgb2, Pdgfrb, Itga8, Actg1, Arhgef7, Mapk3, Ssh3, Cyfip2, Mras, Fgd1, Rac2, Pak3, Myl2, Pdgfa, Pfn2, Itgam, Myl12b, Myh14, Itga4, Myl9, Ppp1cc, Pak6, Pip4k2c, Myh9, Pik3r3, Pdgfc, Fgf8, Sos2, Bdkrb2, Git1, Rras, Nckap1l, Pik3cd, 2900073G15Rik, Itgb3, Fgf18, Chrm3, Tmsb4x, Enah, Rock2, Pip4k2b, Pik3cg, Fgf13, Fgf2, Vav1, Pdgfb, Msn, Myl10, Pak2, Myl7, Csk, Fgf12, Diap1, Itgal, Vav3, Crkl, Dock1, Fgf9, Arpc1b, Slc9a1, Pik3ca, Itga2, Rac3
MMU05340	Primary immunodeficiency	1.8557	0.0016	0.0088	KO	34	22	Blnk, Ighg, Tnfrsf13b, Ada, Cd3d, Ikbkg, Cd40, Jak3, Rfx5, Rfxank, Cd8b1, Rag1, Btk, Tap2, Zap70, Dclre1c, Aicda, Cd8a, Tap1, Ciita, Tnfrsf13c, Il7r
MMU04530	Tight junction	1.8385	0.0000	0.0092	KO	129	43	Cldn7, Ocln, Cldn8, Prkca, Cldn2, Actg1, Src, Amotl1, Mras, Jam2, Pard6b, Inadl, Cldn6, Hcls1, Prkch, Myl2, Cldn23, Gnai1, Myl12b, Cdk4, Myh14, Myl9, Epb4.1l1, Ppp2r2a, Myh9, Llgl1, Pard6g, Rras, Ctnnb1, Gnai2, Cask, 2900073G15Rik, Yes1, Rab13, Prkcb, Epb4.1l2, Pard6a, Myh2, Myl10, Myh1, Myl7, Ppp2r2b, Cttn
MMU05414	Dilated cardiomyopathy (DCM)	1.8295	0.0000	0.0092	KO	88	21	Itgb8, Lmna, Itga6, Ighg, Tpm4, Lama2, Tgfb3, Tgfb2, Tnnt2, Sgcb, Itga8, Actg1, Adcy6, Myl2,

								Cacna2d4, Adcy7, Itga4, Tpm1, Itgb3, Cacnb2, Atp2a2
MMU05211	Renal cell carcinoma	1.8245	0.0000	0.0091	KO	71	25	Pik3r5, Hgf, Pak1, Tgfb3, Tgfb2, Mapk3, Jun, Vegfc, Slc2a1, Pak3, Pdgfa, Pak6, Pik3r3, Gab1, Sos2, Ets1, Pik3cd, Met, Ep300, Pik3cg, Egln3, Pdgfb, Pak2, Rap1b, Crkl
MMU05142	Chagas disease	1.8021	0.0000	0.0118	KO	103	41	Pik3r5, Gna14, Tgfb3, Tgfb2, Tlr2, Ccl2, Mapk3, Cd3g, Jun, Tgfbr1, Ccl12, Mapk13, Smad3, Cd3d, Gnai1, Serpine1, Ppp2r2a, Ikbkg, Pik3r3, Tlr4, Bdkrb2, Gna15, Tnfrsf1a, Nfkbia, Pik3cd, Gnai2, C1qc, Ccl5, Pik3cg, Irak4, Il6, Gnaq, Ppp2r2b, Ticam1, Ifngr1, Tgfbr2, Pik3ca, C1qa, Il1b, Plcb4, Ppp2r1a
MMU05100	Bacterial invasion of epithelial cells	1.7824	0.0015	0.0136	KO	69	26	Cav1, Pik3r5, Was, Clta, Actg1, Src, 4631416L12Rik, Hcls1, Mad2l2, Cav2, Pik3r3, Gab1, Shc4, Cd2ap, Ctnnb1, Pik3cd, Met, Cdh1, Cblb, Pik3cg, Crkl, Cttn, Dock1, Elmo1, Arpc1b, Pik3ca
MMU05145	Toxoplasmosis	1.7776	0.0000	0.0140	KO	124	46	Itga6, H2-Ab1, H2-Eb1, Pik3r5, H2-Aa, Lama2, Tgfb3, Hspa1a, Tgfb2, Lamc3, H2-Oa, Tlr2, Mapk3, Lamb2, Il10rb, Lamb1-1, Mapk13, Bcl2, Bad, Hspa1b, Gnai1, Lama1, Ikbkg, Cd40, Pik3r3, Tlr4, Pla2g2f, H2-Ob, Hspa2, Tnfrsf1a, H2-DMb2, Nfkbia, Pik3cd, Gnai2, H2-DMa, Birc2, Pik3cg, Irak4, Jak1, Nfkbib, Pla2g3, Hspa8, Lama5, Ifngr1, Map2k6, Lama4
MMU05144	Malaria	1.7687	0.0000	0.0147	KO	46	18	Thbs1, Hgf, Tgfb3, Tgfb2, Itgb2, Tlr2, Ccl2, Vcam1, Thbs2, Ccl12, Comp, Icam1, Cd40, Tlr4, Met, Sdc1, Pecam1, Il6
MMU04060	Cytokine-cytokine receptor interaction	1.7496	0.0000	0.0160	KO	220	56	Ltb, Cxcl14, Cxcr7, Il1rap, Cxcr4, Pf4, Cxcl13, Cx3cr1, Hgf, Prlr, Pdgfra, Pdgfd, Ccr1, Tgfb3, Tgfb2, Ccr2, Osmr, Tnfrsf12a, Cxcl16, Pdgfrb, Ccl2, Cxcl10, Tgfbr1, Il10rb, Ccl12, Csf2ra, Vegfc, Tnfrsf1b, Inhbe, Ccl19, Tnfrsf13b, Ccl27a, Cxcl12, Cx3cl1, Pdgfa, Flt3l, Cxcr2, Bmpr1b, Csf2rb2, Tnfrsf21, Clcf1, Cd40, Cxcr6, Pdgfc, Csf2rb, Ccl6, Ccl8, Cxcr3, Il1r2, Tnfrsf1a, Lepr, Bmpr1a, Cxcr5, Ccr3, Met, Il17ra
MMU05214	Glioma	1.7253	0.0014	0.0200	KO	63	20	Ccnd1, Pik3r5, Camk2b, Pdgfra, Pdgfrb, Prkca, Mapk3, Calm3, Pdgfa, Cdk4, Pik3r3, Shc4, Sos2, Cdkn1a, Pik3cd, Plcg2, Prkcb, Pik3cg, Pdgfb, Camk2a
MMU05218	Melanoma	1.7236	0.0029	0.0196	KO	71	24	Ccnd1, Fgf21, Pik3r5, Hgf, Pdgfra, Pdgfd, Fgfr1, Pdgfrb, Mapk3, Pdgfa, Bad, Cdk4, Pik3r3, Pdgfc, Fgf8, Cdkn1a, Pik3cd, Met, Fgf18, Cdh1, Pik3cg, Fgf13, Fgf2, Pdgfb
MMU05410	Hypertrophic cardiomyopathy (HCM)	1.7094	0.0000	0.0221	KO	81	20	Itgb8, Lmna, Itga6, Tpm4, Lama2, Tgfb3, Tgfb2, Tnnt2, Sgcb, Itga8, Actg1, Myl2, Cacna2d4, Itga4, Tpm1, Itgb3, Cacnb2, Atp2a2, Il6, Ryr2
MMU00290	Valine, leucine and isoleucine biosynthesis	1.6918	0.0140	0.0253	KO	10	9	Lars2, Lars, Pdha2, Iars, Bcat1, Iars2, Vars, Vars2, Pdha1
MMU05220	Chronic myeloid leukemia	1.6750	0.0029	0.0282	KO	72	22	Ccnd1, Pik3r5, Tgfb3, Tgfb2, Mapk3, Ctbp2, Tgfbr1, Smad3, Bad, Cdk4, Gab2, Ikbkg, Hdac2, Pik3r3, Shc4, Sos2, Bcr, Cdkn1a, Nfkbia, Pik3cd, Cblb, Pik3cg
MMU04540	Gap junction	1.6304	0.0028	0.0413	KO	81	29	Gja1, Pdgfra, Pdgfd, Pdgfrb, Prkca, Src, Mapk3, Tubb2b, Adcy6, Adcy7, Pdgfa, Tuba1a, Gnai1, Pdgfc, Sos2, Lpar1, Gnai2, Itpr3, Prkcb, Pdgfb, Gnaq, Gucy1b3, Tuba8, Gucy1a3, Prkacb, Cdk1, Prkg1, Plcb4, Grm5
MMU05322	Systemic lupus erythematosus	1.6289	0.0028	0.0406	KO	74	19	Ighg, H2-Ab1, H2-Eb1, H2-Aa, H2-Oa, Hist2h3c2, Hist1h3f, Fcgr3, Cd28, Cd40, Hist3h2a, H2-Ob, Cd86, H2-DMb2, Fcgr1, Hist2h3c1, C1qc, H2-DMa, Hist1h2be
MMU05222	Small cell lung cancer	1.6066	0.0054	0.0488	KO	83	32	Ccnd1, Itga6, Pik3r5, Lama2, Lamc3, Col4a2, Lamb2, Lamb1-1, Col4a1, Bcl2, Fhit, Cdk4, Lama1, Ikbkg, Pik3r3, Nfkbia, Pik3cd, Apaf1, Birc2, Pik3cg, Lama5, Ccne1, Ccne2, Traf1, Lama4, Pik3ca, Itga2, Col4a4, Casp9, Cks1b, Lamc1, Cdkn2b
MMU04010	MAPK signaling pathway	1.6015	0.0000	0.0496	KO	261	86	Relb, Cd14, Fgf21, Mapkapk3, Pak1, Pdgfra, Tgfb3, Ddit3, Fgfr1, Hspa1a, Tgfb2, Pdgfrb, Prkca, Mapk3, Mknk2, Mapkapk2, Jun, Mras, Ntf3, Tgfbr1, Mapk13, Map4k4, Cdc25b, Rac2, Cacna2d4, Pdgfa, Flna, Map3k1, Dusp6, Srf, Rps6ka3, Hspa1b, Ikbkg, Rasa2, Fgf8, Pla2g2f, Sos2, Arrb1, Hspa2, Il1r2, Tnfrsf1a, Rras, Map3k12, Mef2c, Rps6ka1, Stk3, Gadd45b, Map3k3, Ngf, Fgf18, Cacnb2, Mapkapk5, 2010110P09Rik, Prkcb, Fgf13, Fgf2, Pdgfb, Pla2g3, Ppm1a, Arrb2, Rasgrp4, Pak2, Map3k8, Nfkb2, Hspa8, Map3k5, Fgf12, Rap1b, Mapk8ip1, Crkl, Mapk8ip3, Fgf9, Map2k6, Rps6ka6, Prkacb, Ptprr, Tgfbr2, Il1b, Nfatc2, Rac3, Cacna1b, Nf1, Dusp5, Mapk1, Taok3, Ntrk1
MMU05215	Prostate cancer	1.5962	0.0043	0.0507	KO	89	33	Ccnd1, Pik3r5, Pdgfra, Pdgfd, Fgfr1, Pdgfrb, Mapk3, Bcl2, Pdgfa, Bad, Ikbkg, Pik3r3, Pdgfc, Sos2, Cdkn1a, Ctnnb1, Nfkbia, Pik3cd, Ep300, Pik3cg, Pdgfb, Creb3l2, Creb1, Hsp90aa1, Hsp90ab1, Ccne1, Ccne2, Pik3ca, Igf1r, Casp9, Mapk1, Erbb2, Gsk3b

MMU05416	Viral myocarditis	1.5949	0.0083	0.0501	KO	71	26	Ccnd1, Cav1, Ighg, H2-Ab1, H2-Eb1, H2-Aa, Lama2, Itgb2, H2-Oa, Sgcb, Actg1, Rac2, Icam1, Cd28, Myh14, Myh9, Cd40, H2-Ob, Cd86, Fyn, H2-DMb2, Cd55, H2-DMa, Cxadr, Myh2, Myh1
MMU05412	Arrhythmogenic right ventricular cardiomyopathy (ARVC)	1.5868	0.0071	0.0527	KO	73	15	Itgb8, Lmna, Itga6, Gja1, Lama2, Sgcb, Itga8, Actg1, Cacna2d4, Jup, Itga4, Ctnnb1, Itgb3, Cacnb2, Atp2a2
MMU05213	Endometrial cancer	1.5659	0.0231	0.0622	KO	51	19	Ccnd1, Pik3r5, Mlh1, Mapk3, Bad, Foxo3, Pik3r3, Sos2, Ctnnb1, Pik3cd, Axin2, Cdh1, Pik3cg, Pik3ca, Casp9, Ilk, Mapk1, Erbb2, Gsk3b
MMU05200	Pathways in cancer	1.5638	0.0000	0.0620	KO	316	104	Ccnd1, Mmp2, Itga6, Fgf21, Pik3r5, Hgf, Mlh1, Lama2, Pdgfra, Tgfb3, Fgfr1, Tgfb2, Lamc3, Pdgfrb, Prkca, Ralb, Hhip, Mapk3, Ctbp2, Jun, Col4a2, Lamb2, Tgfbr1, Lamb1-1, Csf2ra, Col4a1, Vegfc, Rac2, Slc2a1, Smad3, Jup, Bcl2, Pdgfa, Flt3l, Bad, Wnt8a, Cdk4, Lama1, Ikbkg, Hdac2, Ppard, Pik3r3, Fgf8, Sos2, Rassf5, Bcr, Cdkn1a, Ctnnb1, Nfkbia, Pik3cd, Met, Fzd1, Mmp9, Ep300, Msh6, Dcc, Fgf18, Ralbp1, Axin2, Cdh1, Plcg2, Cblb, Prkcb, Birc2, Pik3cg, Egln3, Runx1t1, Fgf13, Il6, Fgf2, Pdgfb, Jak1, Nfkb2, Lama5, Fgf12, Hsp90aa1, Hsp90ab1, Sfpi1, Ccne1, Fzd2, Ccne2, Crkl, Wnt4, Traf1, Fgf9, Lama4, Tgfbr2, Pik3ca, Wnt2b, Itga2, Col4a4, Rac3, Pparg, Igf1r, Casp9, Mapk1, Erbb2, Cks1b, Csf3r, Gsk3b, Lamc1, Vhl, Rassf1, Ntrk1
MMU00600	Sphingolipid metabolism	1.5585	0.0176	0.0619	KO	38	13	Gal3st1, Sptlc2, B4galt6, Degs2, Neu1, Smpd3, Glb1, Sgpl1, Ppap2a, Ppap2c, Ugt8a, Neu3, Acer2
MMU04210	Apoptosis	1.5491	0.0057	0.0652	KO	85	27	Prkar2b, Il1rap, Pik3r5, Casp12, Endod1, Bcl2, Bad, Csf2rb2, Capn1, Ikbkg, Pik3r3, Csf2rb, Tnfrsf1a, Nfkbia, Pik3cd, Irak2, Apaf1, Ngf, 2010110P09Rik, Birc2, Pik3cg, Irak4, Ripk1, Prkacb, Pik3ca, Il1b, Casp9
MMU05210	Colorectal cancer	1.5484	0.0105	0.0641	KO	62	25	Ccnd1, Pik3r5, Mlh1, Tgfb3, Tgfb2, Mapk3, Jun, Tgfbr1, Rac2, Smad3, Bcl2, Bad, Pik3r3, Ctnnb1, Pik3cd, Msh6, Dcc, Axin2, Pik3cg, Tgfbr2, Pik3ca, Rac3, Casp9, Mapk1, Gsk3b
MMU04350	TGF-beta signaling pathway	1.5311	0.0136	0.0712	KO	80	30	Thbs1, Tgfb3, Tgfb2, Bmp6, Mapk3, Thbs2, Tgfbr1, Acvr1c, Comp, Inhbe, Smad3, Bmpr1b, Id1, Dcn, Bmpr1a, Ep300, Lefty2, Rock2, Bmp5, Lefty1, Bmpr2, Rbl2, Tgfbr2, Ppp2r1a, Mapk1, Ifng, Rbl1, Smurf2, Bmp8b, Cdkn2b
MMU00590	Arachidonic acid metabolism	1.5256	0.0157	0.0732	KO	73	8	Cyp2b13, Gpx7, Cbr3, Ptgds, Cyp4a14, Gpx3, Cyp4f16, Cyp4a31
MMU04115	p53 signaling pathway	1.5217	0.0191	0.0740	KO	64	22	Ccnd1, Thbs1, Ccng1, Ccnb2, Igfbp3, Chek2, Zmat3, Cdk4, Serpine1, Ccnd2, Rrm2b, Mdm4, Cdkn1a, Gadd45b, Apaf1, Sesn2, Ddb2, Pmaip1, Sesn3, Ccne1, Steap3, Ccne2
MMU04012	ErbB signaling pathway	1.5058	0.0161	0.0790	KO	86	42	Pik3r5, Pak1, Camk2b, Ereg, Prkca, Src, Mapk3, Jun, Btc, Pak3, Bad, Pak6, Pik3r3, Gab1, Shc4, Sos2, Cdkn1a, Pik3cd, Plcg2, Cblb, Prkcb, Pik3cg, Camk2a, Pak2, Nck1, Crkl, Pik3ca, Mapk1, Erbb2, Gsk3b, Erbb4, Nrg3, Pak4, Hbegf, Abl2, Map2k1, Camk2d, Eif4ebp1, Mapk9, Nras, Cbl, Grb2
MMU05212	Pancreatic cancer	1.4749	0.0273	0.0981	KO	70	26	Ccnd1, Pik3r5, Tgfb3, Tgfb2, Ralb, Mapk3, Tgfbr1, Vegfc, Rac2, Smad3, Pld1, Bad, Cdk4, Ikbkg, Pik3r3, Pik3cd, Ralbp1, Pik3cg, Jak1, Tgfbr2, Pik3ca, Rac3, Casp9, Mapk1, Erbb2, Arhgef6
MMU00604	Glycosphingolipid biosynthesis - ganglio series	1.4602	0.0637	0.1071	KO	15	5	St3gal2, Hexb, St3gal5, Glb1, St6galnac4
MMU04520	Adherens junction	1.4422	0.0393	0.1181	KO	73	24	Fgfr1, Was, Actg1, Src, Mapk3, Snai2, Tgfbr1, Pvrl1, Rac2, Smad3, Pvrl2, Snai1, Fyn, Ctnnb1, Met, Ep300, Cdh1, Yes1, Ptprm, Tgfbr2, Rac3, Igf1r, Mapk1, Erbb2
MMU00603	Glycosphingolipid biosynthesis - globo series	1.4309	0.0961	0.1239	KO	15	6	St3gal2, Hexb, Fut1, Sec1, A4galt, Naga
MMU04114	Oocyte meiosis	1.4304	0.0253	0.1223	KO	109	37	Rec8, Cpeb1, Camk2b, Ccnb2, Mapk3, Adcy6, Calm3, Spdye4, Adcy7, Mad2l2, Cdc20, Rps6ka3, Anapc10, Ywhab, Ppp1cc, Anapc1, Espl1, Rps6ka1, Itpr3, Ywhah, Ywhag, 2010110P09Rik, Camk2a, Ywhaq, Ccne1, Ccne2, Rps6ka6, Prkacb, Cdk1, Ppp2r1a, Ywhaz, Igf1r, Anapc4, Mapk1, Ppp1ca, Ccnb1, Mad2l1
MMU00601	Glycosphingolipid biosynthesis - lacto and neolacto series	1.4270	0.0740	0.1214	KO	25	10	B3galt2, Fut1, Gcnt2, B4galt4, St3gal4, Sec1, Ggta1, B4galt1, B4galt2, Fut4
MMU05223	Non-small cell lung cancer	1.4224	0.0516	0.1233	KO	54	20	Ccnd1, Pik3r5, Prkca, Mapk3, Bad, Fhit, Foxo3, Cdk4, Pik3r3, Sos2, Rassf5, Pik3cd, Plcg2, Prkcb, Pik3cg, Pik3ca, Casp9, Mapk1, Erbb2, Rassf1
MMU00565	Ether lipid metabolism	1.3998	0.0706	0.1380	KO	34	11	Pafah1b3, Pld1, Pafah1b2, Ppap2a, Ppap2c, Lpcat2, Pla2g2f, Lpcat1, Pafah1b1, Pla2g3, Cept1
MMU04370	VEGF signaling pathway	1.3982	0.0388	0.1356	KO	75	22	Pik3r5, Mapkapk3, Prkca, Src, Mapk3, Mapkapk2, Mapk13, Rac2, Bad, Pik3r3, Pla2g2f, Pik3cd,

								Plcg2, 2010110P09Rik, Prkcb, Pik3cg, Pla2g3, Pik3ca, Nfatc2, Rac3, Casp9, Mapk1
MMU04144	Endocytosis	1.3711	0.0218	0.1601	KO	200	65	Cav1, Nedd4l, Cxcr4, Fam125b, Pdgfra, Tgfb3, Chmp4c, Hspa1a, Tgfb2, Clta, Src, Vps4a, Tgfbr1, Pard6b, Rab31, Ehd2, Ehd4, Smad3, Pld1, Cxcr2, Cav2, Hspa1b, Ehd1, Vps37c, Adrb2, Arrb1, Hspa2, Pard6g, Git1, Rab5c, Rab11fip5, Ap2b1, Arap3, Met, Chmp1a, Rab11fip3, Zfyve20, Agap1, Cblb, Psd4, Vps24, Sh3kbp1, Rab11b, Pard6a, Il2rb, Arrb2, Smap1, Hspa8, Ap2a2, Arfgap1, Tgfbr2, Sh3gl1, Igf1r, Tfrc, Agap2, Pld2, Flt1, Ntrk1, Erbb4, Iqsec3, Smurf2, Prkci, Rab22a, Fgfr4, Pip5k1c
MMU03430	Mismatch repair	1.3375	0.1347	0.1923	KO	22	13	Mlh1, Rpa2, Exo1, Msh6, Rfc2, Pold4, Pcna, Lig1, Pold2, Pold3, Rfc3, Pms2, Rpa1
MMU00480	Glutathione metabolism	1.3320	0.0854	0.1963	KO	52	11	Gpx7, Gpx3, Mgst2, Gstm2, Gstm3, Ggt6, Rrm2b, Gstm5, Mgst3, G6pdx, Ggt5
MMU04110	Cell cycle	1.3303	0.0446	0.1954	KO	122	45	Ccnd1, Tgfb3, Ccnb2, Tgfb2, Cdkn2c, Cdkn1c, Cdc25b, Fzr1, Smad3, Chek2, Mad2l2, Cdc20, Anapc10, Cdk4, Orc2l, Ywhab, Bub1b, Hdac2, Ccnd2, Anapc1, Cdkn1a, Espl1, Ep300, Gadd45b, Ywhah, Ywhag, Cdc25a, Ywhaq, Cdc14a, Ccna2, Cdk7, Pcna, Ccne1, Ccne2, Rbl2, Orc3l, Cdk1, Ywhaz, Anapc4, Rad21, Gsk3b, Rbl1, Cdkn2b, Ccnb1, Mad2l1
MMU00790	Folate biosynthesis	1.3081	0.1615	0.2169	KO	11	1	Alpl
MMU00750	Vitamin B6 metabolism	1.2872	0.1537	0.2365	KO	6	3	Psat1, Pnpo, Pdxp
MMU05219	Bladder cancer	1.2871	0.1234	0.2338	KO	41	9	Ccnd1, Mmp2, Thbs1, Mapk3, Vegfc, Cdk4, Cdkn1a, Mmp9, Cdh1
MMU00982	Drug metabolism - cytochrome P450	1.2867	0.1149	0.2315	KO	65	7	Cyp2b13, Fmo3, Fmo2, Mgst2, Fmo4, Gstm2, Gstm3
MMU00520	Amino sugar and nucleotide sugar metabolism	1.2801	0.1216	0.2374	KO	46	13	Gnpda2, Gnpda1, Uap1l1, Hexb, Nagk, Hk1, Gmppa, Pgm1, Pgm3, Npl, Gfpt1, Gne, Mpi
MMU04130	SNARE interactions in vesicular transport	1.2785	0.1357	0.2368	KO	35	8	Vamp3, Stx6, Bet1l, Snap29, Stx11, Stx2, Gosr2, Ykt6
MMU04146	Peroxisome	-1.3769	0.0400	0.3918	WT	78	30	Slc27a2, Nudt12, Pex11c, Pex1, Pxmp2, Cat, Dhrs4, Acox2, Mlycd, Ehhadh, Acox3, Acsl5, Amacr, Ephx2, Dao, Pex11a, Pex16, Hsd17b4, Sod2, Acsl6, Hao1, Decr2, Pecr, Mpv17l, Mvk, Acaa1b, Abcd2, Idh1, Pmvk, Scp2
MMU00900	Terpenoid backbone biosynthesis	-1.8799	0.0026	0.0158	WT	14	8	Mvk, Mvd, Acat2, Fdps, Idi1, Pmvk, Hmgcr, Hmgcs1
MMU00120	Primary bile acid biosynthesis	-1.9265	0.0024	0.0108	WT	15	9	Cyp8b1, Cyp46a1, Baat, Slc27a5, Acox2, Cyp27a1, Amacr, Hsd17b4, Cyp7a1
MMU00100	Steroid biosynthesis	-2.1391	0.0000	0.0017	WT	18	3	Cel, Hsd17b7, Sqle

*CGU00001: A curated list of liver fibrotic genes (Gutiérrez-Ruiz, et al., 2007; Friedman 2008; Bosselut et al., 2010)

NES: normalized enrichment score with positive and negative enrichment scores indicating correlation and anti-correlation with mir-122 knockout phenotype, respectively.

FDR: false detection rate.

P: nominal *P* value.

Supplementary Table 5. Relative expression levels of genes in KEGG "Pathway in cancer" gene set

Gene Symbol	2 month KO/WT		11-month KO-T/WT		14-month KO-T/WT	
	Fold-Change	p-value *	Fold-Change	p-value *	Fold-Change	p-value *
Lef1	-1.00	0.9937	1.04	0.9588	-3.81	0.0368
Abl1	-1.42	0.5970	-1.60	0.4978	-2.23	0.0130
Runx1	1.19	0.7158	-1.45	0.2121	-3.51	0.0035
Wnt8a	1.25	0.6128	-1.01	0.9749	-3.60	0.0467
E2f1	1.36	0.6599	-1.42	0.4926	-3.39	0.0093
Ptch1	1.11	0.7595	-1.21	0.4086	-5.15	0.0049
Ntrk1	1.57	0.3515	-1.62	0.5286	-2.21	0.0297
Fzd10	-1.22	0.5763	-1.98	0.2710	-2.96	0.0072
Pax8	-1.20	0.7203	-2.77	0.0951	-2.73	0.0137
Wnt2	-1.10	0.5226	-1.83	0.2022	-2.57	0.0242
Axin2	-1.01	0.9730	-3.13	0.0124	-2.07	0.0102
Map2k2	1.73	0.0925	-2.19	0.2343	-2.85	0.0177
Pik3cb	1.02	0.9300	-2.50	0.2774	-3.13	0.0149
Bmp2	-1.06	0.7104	-3.01	0.2295	-3.72	0.0078
Cdh1	1.42	0.0606	-1.35	0.5878	-2.50	0.0136
Rxrg	-1.30	0.6610	-2.75	0.3143	-2.15	0.0363
Ikbkb	1.12	0.8191	-2.06	0.4340	-3.13	0.0111
Fzd8	-1.54	0.1649	-1.84	0.4194	-5.33	0.0010
Tcf7l2	-1.50	0.1524	-2.15	0.1903	-3.69	0.0350
Cebpa	1.00	0.9983	-2.74	0.2044	-3.72	0.0107
Wnt9a	-1.18	0.7724	-1.44	0.4010	-3.00	0.0327
Wnt8b	-2.18	0.0949	-2.17	0.4091	-3.09	0.0089
Nos2	1.32	0.3145	3.19	0.1914	-3.52	0.0040
Fzd6	-2.25	0.2104	1.01	0.9751	-3.87	0.0091
Fgf10	-1.98	0.4092	1.20	0.7459	-2.28	0.0329
Fn1	-2.92	0.1627	-1.80	0.0002	-2.58	0.0096
Wnt16	-2.26	0.2372	-1.14	0.7458	-2.20	0.0293
Pias2	-1.34	0.4743	-2.34	0.2887	-3.17	0.0428
Chuk	-1.67	0.3334	-2.23	0.3575	-2.91	0.0059
Vamp7	-2.01	0.2909	-2.69	0.0910	-3.66	0.0001
Xiap	-1.70	0.3730	-2.82	0.1210	-3.47	0.0007
Ctnna3	-1.43	0.3727	-3.23	0.0195	-3.33	0.0008
Egfr	-1.47	0.0250	-2.98	0.0534	-4.18	0.0002
Fgf1	-1.95	0.0061	-2.43	0.0002	-4.65	0.0029
Sos1	-1.53	0.2948	-4.74	0.0483	-2.71	0.0213
Stat5b	-2.66	0.0014	-2.69	0.1896	-2.79	0.0303
Rad51	1.13	0.4269	1.56	0.5724	3.40	0.0111
Birc5	1.26	0.1015	1.33	0.7433	3.43	0.0044
Cks1b	1.57	0.1427	1.38	0.6784	3.53	0.0393
Smad2	1.21	0.7087	-1.06	0.9574	2.97	0.0069
Lamb3	-1.41	0.2774	2.85	0.2053	2.27	0.0363
E2f3	-1.85	0.1112	-1.15	0.8103	3.17	0.0488
Lamb2	1.31	0.1156	1.69	0.1405	3.34	0.0017
Tpr	1.04	0.8971	1.91	0.0855	3.86	0.0003
Skp2	-1.08	0.7968	-1.04	0.9393	3.25	0.0348
Gsk3b	1.29	0.2899	1.66	0.2111	3.46	0.0085
Tgfbr2	1.67	0.0814	2.13	0.0910	3.80	0.0003
Egln3	1.34	0.0975	3.09	0.0737	5.08	0.0001
Cdc42	1.36	0.1314	2.60	0.1104	4.08	0.0019
Sos2	1.87	0.2385	1.93	0.0554	3.21	0.0178
Cdkn1a	1.07	0.8888	2.90	0.0756	3.45	0.0068
Bax	1.59	0.2257	2.08	0.3080	3.64	0.0030
Ep300	2.59	0.0016	1.76	0.1859	4.10	0.0032
Rbx1	1.60	0.0217	2.21	0.0874	3.93	0.0076
Cdkn2b	1.54	0.1881	2.02	0.2487	4.42	0.0069
Itga6	1.53	0.0961	2.70	0.1392	4.41	0.0018
Ralb	1.78	0.0014	3.19	0.0192	4.73	0.0002
Pdgfb	1.27	0.0207	3.22	0.1492	3.65	0.0173
Col4a2	1.55	0.0520	3.63	0.0987	4.24	0.0029
Col4a1	1.51	0.0460	4.07	0.0308	4.85	0.0007
Slc2a1	1.46	0.0392	2.24	0.2130	4.10	0.0117
Raf1	1.23	0.1339	1.78	0.4081	3.34	0.0327
Stat1	-1.58	0.0055	2.00	0.3618	3.66	0.0042
Itgav	1.06	0.5898	2.93	0.1185	3.73	0.0013
Wnt4	1.07	0.4217	2.12	0.2401	3.77	0.0299
Sars	1.73	0.0028	3.11	0.0776	3.66	0.0317
Cdk4	1.81	0.0377	3.29	0.1271	3.52	0.0255
Pik3ca	1.09	0.8721	3.22	0.1558	2.56	0.0370
Bad	2.50	0.2610	1.75	0.2699	2.03	0.0294
Pak6	1.72	0.0343	2.40	0.0461	4.82	0.0062
Ctnna1	1.77	0.0946	2.48	0.1021	4.33	0.0012
Traf2	1.55	0.1852	3.05	0.0029	5.03	0.0024
Mapk3	2.66	0.0225	4.07	0.0105	3.83	0.0009
Kras	2.09	0.0249	4.19	0.0348	4.18	0.0006
Smad4	1.69	0.0652	1.45	0.5585	5.82	0.0010
Tgfb2	2.20	0.0596	4.42	0.0611	2.61	0.0318

Prkcb	**1.71**	**0.1263**	**4.98**	**0.1204**	**2.41**	**0.0338**
Sfpi1	**1.64**	**0.2466**	**4.66**	**0.0804**	**2.77**	**0.0127**
Bcl2	**2.19**	**0.1253**	**2.65**	**0.1448**	**3.08**	**0.0108**
Map2k1	**1.50**	**0.3769**	**2.37**	**0.2503**	**4.08**	**0.0035**
Pik3r5	**2.43**	**0.0132**	**5.22**	**0.0743**	**2.43**	**0.0017**
Csf2ra	**1.60**	**0.0053**	**4.65**	**0.0551**	**4.09**	**0.0001**
Tgfbr1	**1.44**	**0.1596**	**3.34**	**0.1043**	**4.18**	**0.0002**
Birc2	**2.18**	**0.0051**	**2.06**	**0.4512**	**2.99**	**0.0012**
Nfkb1	**1.28**	**0.2917**	**4.55**	**0.0759**	**3.19**	**0.0116**
Plcg2	**2.02**	**0.0247**	**5.02**	**0.1473**	**2.26**	**0.0314**
Ctbp2	**2.57**	**0.0032**	**3.70**	**0.1341**	**3.35**	**0.0060**
Pdgfrb	**2.65**	**0.0005**	**3.59**	**0.0507**	**3.28**	**0.0353**
Jak1	**2.48**	**0.0020**	**2.88**	**0.1146**	**3.99**	**0.0100**
Lama2	**3.31**	**0.0119**	**2.02**	**0.2691**	**2.43**	**0.0217**
Ikbkg	**2.55**	**0.0267**	**1.12**	**0.8856**	**3.10**	**0.0133**

*** p-value determined by unpaired, two-tailed Student's t-test.**

2 month KO/WT: expression fold-change of 122KO and Wild-type livers.

11-month KO-T/WT: expression fold-change of tumors from 122KO livers and WT livers.

14-month KO-T/WT: expression fold-change of tumors from 122KO livers and WT livers

Supplemental Table 6. Nucleotide positions of the predicted *Mir122a*-binding sites within the 3'UTR of the candidate target genes.

Genes	# Binding sites	Sc-M of each binding site	3'UTR locations¶ of the predicted binding site
1110021L09Rik	4	122.00, 138.00, 120.00, 147.00	294-318, 528-549, 585-612, 1162-1186
1700025G04Rik	2	158.00, 126.00	6633-6657, 8607-8632
4933426M11Rik	4	125.00, 120.00, 131.00, 140.00	1114-1147, 1684-1705, 2618-2642, 2808-2837
AA986860	2	120.00, 153.00	660-681, 696-718
Aak1	8	120.00, 142.00, 130.00, 121.00, 129.00, 127.00, 124.00, 128.00	340-361, 3927-3952, 3989-40105063-5090, 5397-5420, 6070-6092, 9708-9730, 12757-12781
Abcc9	4	137.00, 142.00, 132.00, 138.00	447-471, 620-642, 704-731, 1155-1176
Abhd2	1	136	779-800
Adam10	1	120	36-57
Adamtsl2	1	128	151-170
Adcy6	1	134	2191-2212
Agpat1	6	120.00, 123.00, 120.00, 130.00, 151.00, 131.00	63-84, 111-136, 165-186, 247-272, 441-458, 554-580
Ahr	1	124	35-57
Aldoa	1	148	17-40
Alpl	3	140.00, 140.00, 153.00	295-316, 480-501, 509-529
Amot	1	131	2444-2463
Ankrd13c	3	142.00, 145.00, 139.00	227-251, 279-304, 504-530
Ano6	4	153.00, 131.00, 127.00, 120.00	514-540, 684-705, 1783-1803, 1884-1905
Arfip2	2	121.00, 151.00	233-260, 264-310
Arhgap1	3	122.00, 120.00, 157.00	521-552, 584-605, 1231-1252
Arl2	1	152	56-85
Arl8b	1	133	1375-1402
Asb1	3	136.00, 148.00, 148.00	171-191, 771-800, 3554-3571
Atp11a	6	140.00, 150.00, 135.00, 130.00, 156.00, 128.00	672-691, 960-985, 1831-1852, 1953-1979, 2018-2046, 3499-3524
Atp1b1	1	164	518-540
Atp6v0a2	2	123.00, 121.00	36-75, 164-191
Atp6v0e2	4	123.00, 144.00, 120.00, 123.00	292-309, 544-569, 695-716, 726-746
Atp7a	2	120.00, 128.00	1382-1403, 2750-2776
Atpbd4	4	148.00, 139.00, 146.00, 160.00	228-248, 403-425, 1347-1373, 1402-1420
Atpif1	1	120	25-46
AU040320	3	120.00, 125.00, 124.00	101-122, 269-291, 601-623
AU040829	1	136	80-102
B230208H17Rik	3	134.00, 124.00, 157.00	317-333, 664-687, 974-997
Bcat2	1	151	126-155
Btla	1	146	1894-1930
Card10	1	126	1165-1191
Cav2	2	127.00, 135.00	421-441, 891-917
Cbx5	4	135.00, 123.00, 153.00, 151.00	2682-2707, 4324-4349, 7203-7221, 7529-7554
Ccdc3	3	127.00, 121.00, 124.00	1183-1205, 1425-1455, 1539-1560
Ccnd1	1	120	514-535
Ccnd2	3	136.00, 156.00, 126.00	2939-2966, 2987-3008, 3134-3152
Ccnyl1	3	120.00, 153.00, 124.00	209-230, 630-653, 1060-1083
Ccr2	1	160	856-885
Ccrn4l	2	120.00, 140.00	67-103, 147-178
Cd320	2	148.00, 154.00	154-181, 260-284
Cda	2	130.00, 129.00	137-160, 206-237
Cdc42ep1	1	128	227-261
Cdh1	1	127	116-143
Cldn2	2	126.00, 120.00	1224-1262, 1703-1724
Cldn7	1	120	37-60
Clic1	1	163	69-92
Clic4	3	154.00, 126.00, 143.00	138-162, 1560-1593, 2629-2655
Clic5	2	124.00, 155.00	2037-2065, 4569-4594
Col3a1	1	143	273-293
Cpeb1	2	144.00, 156.00	356-377, 581-602
Cpne8	1	126	10-37
Crispld2	5	152.00, 144.00, 134.00, 140.00, 120.00	276-297, 518-539, 586-608, 905-924,1741-1762
Cs	1	146	1150-1173

Csnk1g1	6	134.00, 128.00, 121.00, 131.00, 122.00, 144.00	1647-1675, 2663-2690, 4250-4273, 4301-4321, 4555-4573, 4839-4871
Ctps2	2	140.00, 121.00	792-815, 1327-1349
Cxcl12	4	145.00, 125.00, 135.00, 123.00	166-187, 886-914, 1722-1746, 4167-4186
Cybb	1	130	946-969
Cygb	1	147	224-246
Ddit4l	1	140	1091-1119
Ddr1	1	151	155-175
Ddr2	1	120	65-86
Dlat	2	154.00, 145.00	184-212, 1397-1424
Dock5	4	154.00, 144.00, 138.00, 129.00	405-424, 830-852, 3384-3406, 4358-4382
Dpt	2	135.00, 133.00	86-102, 200-224
Dynll1	1	132	727-750
Elovl1	1	127	188-209
Emilin1	1	120	112-137
Emp1	1	128	1070-1094
Enc1	2	139.00, 134.00	148-169, 1303-1324
Endod1	2	155.00, 122.00	1847-1870, 2277-2306
Enpp5	2	155.00, 124.00	153-179, 402-426
Erlin2	2	122.00, 161.00	77-98, 636-653
Ezr	2	127.00, 134.00	28-61, 794-820
Fam149a	2	139.00, 123.00	348-386, 1308-1330
Fam49b	2	123.00, 148.00	1858-1879, 2260-2282
Fam82a2	1	136	514-540
Fbln5	2	139.00, 157.00	3088-3112, 3474-3508
Fgfr1	1	127	1194-1215
Flnb	3	124.00, 135.00, 140.00	112-134, 421-441, 503-535
Fmo2	2	123.00, 158.00	539-566, 1490-1516
Fuca2	2	147.00, 126.00	299-317, 1465-1486
G3bp2	4	137.00, 145.00, 127.00, 124.00	649-671, 806-827, 1229-1250, 1642-1662
G6pc3	1	151	18-62
Gabra3	1	135	1344-1367
Gde1	2	128.00, 120.00	50-71, 286-323
Gfpt1	3	136.00, 123.00, 154.00	369-391, 680-706, 1874-1912
Ggps1	1	148	114-140
Gja1	2	124.00, 144.00	466-487, 1585-1611
Glyctk	1	128	780-830
Gmppa	1	145	24-45
Gnpda1	3	130.00, 161.00, 130.00	487-514, 780-802, 955-971
Gnpda2	2	142.00, 146.00	143-171, 332-361
Golph3l	5	128.00, 135.00, 151.00, 154.00, 131.00	92-120, 399-431, 532-553, 583-608, 1063-1083
Gpm6b	1	172	54-74
Gpr107	1	150	77-110
Gpr172b	1	163	109-132
Gys1	3	120.00, 154.00, 136.00	70-97, 131-154, 160-191
Hhip	10	127.00, 130.00, 132.00, 141.00, 145.00, 138.00, 122.00, 120.00, 138.00, 120.00	460-480, 908-926, 1157-1179, 1372-1398, 1844-1860, 2937-2969, 3423-3454, 3476-3501, 3659-3684, 5554-5591
Idh3a	4	120.00, 154.00, 120.00, 157.00	22-46, 274-293, 700-721, 783-803
Idh3g	1	136	41-63
Igf2	4	120.00, 140.00, 129.00, 120.00	90-111, 930-955, 2115-2137, 2298-2319
Igfbp7	1	138	65-86
Ikbkg	8	124.00, 143.00, 159.00, 124.00, 121.00, 120.00, 159.00, 127.00	65-91, 776-796, 943-968, 1038-1059, 1748-1763, 1869-1890, 4228-4259, 5338-5359
Ints2	1	127	1343-1362
Itgb8	1	128	269-317
Jdp2	2	128.00, 128.00	236-260, 308-325
Jun	1	140	860-883
Kbtbd11	2	123.00, 130.00	75-96, 4529-4564
Kctd17	1	147	162-183
Klf6	1	158	953-976
Lars2	1	161	586-610
Lass6	3	124.00, 120.00, 148.00	281-303, 1498-1519, 2004-2024
Lcmt1	1	122	180-204
Leprot	2	122.00, 120.00	154-178, 324-346
Lhfp	1	136	406-427
Limd2	1	135	811-843
Lpar1	1	140	76-115
Lpcat3	2	138.00, 128.00	52-76, 87-119
Lpl	1	155	1460-1484
Lztfl1	4	133.00, 143.00, 136.00, 140.00	208-235, 1048-1071, 1148-1169,

			2054-2075
Maf1	1	148	316-334
Maged2	2	142.00, 138.00	287-312, 324-348
Map3k1	1	139	1577-1603
Map4k4	1	127	1472-1491
Mapk3	2	132.00, 139.00	163-189, 391-421
Mapkapk2	2	124.00, 120.00	270-297, 879-907
Mapre1	5	132.00, 135.00, 140.00, 140.00, 134.00	61-84, 90-112, 874-895, 2248-2270, 3273-3294
Marcks	1	132	3501-3526
Mast2	1	128	22-48
Mcrs1	1	149	226-255
Med28	3	127.00, 131.00, 150.00	915-950, 2154-2170, 3917-3936
Mfge8	1	145	383-400
Mfsd11	4	120.00, 140.00, 132.00, 127.00	337-358, 496-520, 679-697, 884-906
Mknk2	1	120	302-323
Mlec	3	143.00, 120.00, 120.00	365-384, 2426-2447, 4843-4864
Mmp2	1	124	503-524
Mras	4	130.00, 133.00, 120.00, 144.00	506-529, 1199-1219, 2146-2173, 2182-2205
Mrs2	1	145	376-397
Mtmr11	1	122	69-93
Mtpn	1	131	576-594
Myo5b	1	144	986-1008
Naaa	1	160	252-273
Nap1l1	3	132.00, 142.00, 120.00	1241-1267, 1521-1552, 1857-1882
Ndrg3	3	120.00, 151.00, 156.00	36-57, 182-207, 1251-1278
Necap2	3	131.00, 141.00, 135.00	150-182, 196-218, 387-406
Nedd9	1	148	1571-1593
Nf2	4	122.00, 144.00, 158.00, 123.00	396-424, 729-750, 999-1025, 2271-2290
Nfe2l1	1	124	737-762
Nfkbiz	1	120	1276-1303
Nid1	2	147.00, 120.00	31-52, 953-974
Nkd1	3	123.00, 132.00, 154.00	446-467, 871-892, 1179-1203
Nrxn1	3	132.00, 129.00, 140.00	3219-3257, 3292-3317, 3370-3392
Ntrk2	6	120.00, 135.00, 132.00, 121.00, 145.00, 134.00	1317-1338, 1541-1559, 2061-2086, 3122-3145, 3960-3987, 4483-4504
Nupl1	1	135	102-129
Obfc1	1	165	319-348
Ocln	2	143.00, 120.00	191-220, 332-372
Oxct1	3	129.00, 120.00, 120.00	450-471, 1006-1035, 1173-1194
P4ha1	3	149.00, 152.00, 130.00	74-95, 1768-1790, 2187-2219
Parp3	1	129	254-282
Pdgfra	1	122	2844-2894
Pdgfrb	2	120.00, 144.00	615-636, 985-1012
Pfkfb3	2	120.00, 126.00	1058-1079, 2263-2290
Pip4k2a	2	139.00, 151.00	218-242, 534-556
Pldn	3	120.00, 133.00, 134.00	695-720, 1376-1396, 1522-1550
Plp2	1	148	177-202
Plscr1	1	123	137-165
Plscr3	4	167.00, 136.00, 144.00, 150.00	259-279, 1044-1071, 1445-1465, 1471-1490
Plxna1	4	120.00, 150.00, 130.00, 151.00	573-594, 1544-1577, 2400-2429, 2827-2847
Pnpla6	1	148	64-103
Ppapdc1b	2	121.00, 136.00	241-283, 385-406
Ppl	1	124	768-808
Ppp1cc	1	157	535-559
Ppp1r10	2	136.00, 123.00	199-219, 665-686
Prkcb	5	136.00, 132.00, 133.00, 132.00, 127.00	1484-1506, 1508-1533, 3001-3020, 3826-3843, 4858-4878
Prlr	12	134.00, 148.00, 128.00, 134.00, 143.00, 133.00, 130.00, 120.00, 138.00, 159.00, 120.00, 127.00	149-167, 489-507, 538-564, 1675-1698, 2514-2534, 2850-2866, 2941-2967, 3375-3395, 5462-5483, 5749-5773, 6798-6826, 7242-7265
Ptdss2	1	147	99-118
Pxmp4	1	162	125-150
Pycrl	1	151	345-373
Rad51l1	1	127	619-651
Ralb	2	144.00, 149.00	1109-1137, 1186-1202
Rbms3	1	148	5360-5385
Rcan1	1	128	581-602
Rell1	2	137.00, 142.00	264-285, 736-753
Rhob	1	132	913-937
Rnf38	6	130.00, 140.00, 132.00, 160.00, 153.00, 136.00	234-261, 646-668, 773-794, 1203-1225, 2919-2943, 3359-3380
Rogdi	1	146	225-255

Rtn3	1	158	1571-1595
Sav1	1	124	1029-1050
Sbk1	6	144.00, 136.00, 125.00, 156.00, 122.00, 125.00	238-256, 613-635, 673-693, 855-887, 1178-1205, 2213-2242
Scara3	2	121.00, 148.00	796-819, 1090-1135
Serpine2	1	132	392-413
Serpinh1	2	120.00, 122.00	158-181, 394-415
Sesn2	1	134	409-434
Shb	1	131	549-569
Slc10a3	1	131	24-46
Slc1a4	6	124.00, 124.00, 138.00, 141.00, 138.00, 130.00	159-180, 627-650, 812-835, 1105-1129, 1184-1208, 1448-1468
Slc25a34	3	160.00, 139.00, 159.00	2010-2031, 2040-2062, 2187-2207
Slc2a1	2	122.00, 143.00	268-287, 709-727
Slc35a4	4	139.00, 125.00, 141.00, 124.00	198-218, 328-347, 518-539, 598-619
Slc39a3	2	152.00, 139.00	2075-2098, 2285-2330
Slc43a2	1	140	451-477
Slc5a1	2	146.00, 130.00	183-206, 983-1007
Slc6a8	3	134.00, 122.00, 132.00	686-712, 883-909, 1281-1309
Slc7a7	1	126	221-249
Smap1	3	131.00, 152.00, 123.00	94-110, 262-284, 537-554
Snap29	4	126.00, 123.00, 147.00, 120.00	349-371, 903-937, 1326-1347, 2098-2119
Snx18	2	126.00, 132.00	415-436, 834-859
Snx6	1	140	178-201
Sox4	1	120	242-274
Sox6	5	130.00, 120.00, 120.00, 137.00, 147.00	14-35, 2665-2701, 2848-2872, 3695-3721, 5512-5534
Sparc	1	131	571-592
Sptlc2	3	133.00, 122.00, 144.00	93-115, 158-174, 1668-1695
Src	1	129	1780-1801
St3gal2	2	136.00, 121.00	342-364, 485-512
Stk24	1	149	647-667
Stx3	1	124	107-128
Synpo	4	120.00, 120.00, 122.00, 140.00	559-580, 939-960, 1355-1372, 1846-1870
Taf1	2	152.00, 130.00	197-222, 1920-1952
Tagln2	2	127.00, 120.00	53-79, 454-478
Tead1	6	143.00, 132.00, 124.00, 122.00, 131.00, 143.00	37-68, 2556-2577, 3260-3287, 3782-3806, 5527-5546, 6395-6416
Tecpr1	1	127	409-432
Tgfbr2	2	126.00, 135.00	1292-1312, 2514-2535
Thbs1	2	132.00, 120.00	887-908, 1348-1369
Tmem175	2	151.00, 147.00	635-657, 925-951
Tmem20	5	139.00, 145.00, 122.00, 151.00, 121.00	852-876, 914-936, 1358-1383, 1528-1556, 1874-1894
Tmem41b	3	130.00, 158.00, 126.00	19-41, 2054-2075, 2480-2524
Tmem43	3	120.00, 138.00, 154.00	48-74, 494-519, 871-896
Tmem50b	3	156.00, 135.00, 144.00	558-583, 872-895, 1257-1279
Tmprss2	1	128	1215-1243
Tnfrsf1b	3	133.00, 137.00, 139.00	772-795, 1691-1712, 2242-2276
Tnrc6c	2	146.00, 127.00	602-626, 2266-2293
Tspyl1	3	154.00, 123.00, 120.00	457-489, 502-523, 641-662
Ttc39a	2	127.00, 129.00	77-97, 412-439
Uba6	2	140.00, 126.00	1-25, 977-999
Ucp2	3	121.00, 148.00, 138.00	514-553, 1996-2018, 2793-2824
Usp22	3	135.00, 151.00, 138.00	100-118, 1761-1780, 1959-1985
Vamp3	2	149.00, 124.00	146-178, 598-621
Vcam1	1	127	288-318
Vps4a	3	162.00, 123.00, 127.00	205-232, 347-369, 415-435
Wars	2	162.00, 122.00	36-63, 788-813
Wnk2	2	127.00, 120.00	11-33, 54-75
Wwtr1	4	162.00, 132.00, 134.00, 144.00	104-136, 2133-2152, 2693-2724, 3098-3119
Zbtb4	7	145.00, 135.00, 146.00, 124.00, 120.00, 123.00, 123.00	93-111, 433-453, 848-873, 1027-1056, 1668-1689, 3044-3064, 4490-4514
Zbtb45	2	125.00, 120.00	5-28, 43-64
Zdhhc24	2	132.00, 162.00	954-979, 1249-1268
Zfp106	2	122.00, 147.00	620-647, 663-685
Zfp426	4	135.00, 120.00, 164.00, 140.00	145-161, 408-435, 473-497, 577-599
Zfp704	6	124.00, 150.00, 131.00, 166.00, 124.00, 124.00	1829-1850, 7600-7623, 8345-8361, 9247-9273, 9410-9431, 10699-10721

[¶], positions of *Mir122a*-binding sites in the 3'UTR (the nucleotide after the stop codon is numbered as #1)

Supplemental Table 7. Experimentally verified *MIR122*/*Mir122a* target genes.

Target genes	Species	Validation methods	Refs.
Functional miRNA-target interactions (Positive samples)			
AACS	H. sapiens	Reporter assay; qRT-PCR	15
ADAM10	H. sapiens	Reporter assay	67
ADAM17	H. sapiens	Reporter assay; qRT-PCR	15
AKT3	H. sapiens	Reporter assay; qRT-PCR	15
ALDOA	H. sapiens; M. musculus	Reporter assay; Western blot; qRT-PCR	5, 6, 15, 38, 66, 73
Alpl	M. musculus	Reporter assay	This study
ANK2	H. sapiens	Reporter assay; qRT-PCR	15
ANXA11	H. sapiens	Reporter assay; qRT-PCR	15
AP3M2	H. sapiens	Reporter assay; qRT-PCR	15
Apob	M. musculus	Western blot	6
ATP1A2	H. sapiens	Reporter assay; qRT-PCR	15
Bach1	M. musculus	qRT-PCR	67
Bckdk	M. musculus	Reporter assay; Western blot; qRT-PCR	38
BCL2L2	H. sapiens	Reporter assay; Western blot; qRT-PCR	68, 71
CCNG1	H. sapiens; M. musculus	Reporter assay; qRT-PCR	6, 68, 69, 71
Ccrn4L	M. musculus	Reporter assay; Western blot; qRT-PCR	70
Cd320	M. musculus	Reporter assay; Western blot; qRT-PCR	38
CLIC4	H. sapiens	Reporter assay	71
Cs	M. musculus	Reporter assay	This study
CTCF	H. sapiens	Reporter assay	71
CUX1	H. sapiens	Reporter assay	71
CYP7A1	H. sapiens	Reporter assay; qRT-PCR	72
Ddc	M. musculus	Reporter assay	8
DSTYK	H. sapiens	Reporter assay; qRT-PCR	15
DUSP2	H. sapiens	Reporter assay; qRT-PCR	15
EGLN3	H. sapiens	Reporter assay; qRT-PCR	15
ENTPD4	H. sapiens	Reporter assay; qRT-PCR	15
FAM117B	H. sapiens	Reporter assay; qRT-PCR	15
FOXJ3	H. sapiens	Reporter assay; qRT-PCR	15
FOXP1	H. sapiens	Reporter assay; qRT-PCR	15
FUNDC2	H. sapiens	Reporter assay; qRT-PCR	15
G6PC3	H. sapiens	Reporter assay; qRT-PCR	15
GALNT10	H. sapiens	Reporter assay; qRT-PCR	15
Gpx7	M. musculus	Reporter assay	73
GTF2B	H. sapiens	qRT-PCR	66
GYS1	H. sapiens; M. musculus	Western blot; qRT-PCR	6, 66
Hfe2	M. musculus	Reporter assay	5, 73
Hist1H1C	M. musculus	Reporter assay	8
IGF1R	H. sapiens	Reporter assay	65
Klf6	M. musculus	Reporter assay	This study
LAMC1	H. sapiens	Reporter assay	71
Lass6	M. musculus	Reporter assay	73
MAP3K12	H. sapiens	Reporter assay	71
MAP3K3	H. sapiens	Reporter assay	71
MAPK11	H. sapiens	Reporter assay; qRT-PCR	15
MARK1	H. sapiens	Reporter assay	71
MECP2	H. sapiens	Reporter assay; qRT-PCR	15
NCAM1	H. sapiens	Reporter assay; qRT-PCR	15
Ndrg3	M. musculus	Reporter assay; Western blot; qRT-PCR	5, 38
NFATC2IP	H. sapiens	Reporter assay; qRT-PCR	15
NUMBL	H. sapiens	Reporter assay; qRT-PCR	15

P4Ha1	M. musculus	qRT-PCR	6
Ppard	M. musculus	Reporter assay	8
Prom1	M. musculus	Reporter assay	This study
RAB11FIP1	H. sapiens	Reporter assay; qRT-PCR	15
RAB6B	H. sapiens	Reporter assay; qRT-PCR	15
RAD21	H. sapiens	Reporter assay	71
Rcan1	M. musculus	Reporter assay	8
Rell1	M. musculus	Reporter assay	8
RHOA	H. sapiens	Reporter assay	16
Sbk1	M. musculus	Reporter assay	8
Slc35A4	M. musculus	Reporter assay	5, 73
SLC7A1	H. sapiens; M. musculus	Reporter assay; Western blot; qRT-PCR	6, 15, 16, 66, 73
SLC7A11	H. sapiens	Reporter assay; qRT-PCR	15
Smarcd1	M. musculus	Reporter assay	8
Sox4	M. musculus	Reporter assay	This study
SRF	H. sapiens	Reporter assay	65
TBX19	H. sapiens	Reporter assay; qRT-PCR	15
Tgfbr1	M. musculus	Reporter assay	8
Tmed3	M. musculus	Reporter assay	5, 73
Tmem50B	M. musculus	Reporter assay	73
TPD52L2	H. sapiens	Reporter assay; qRT-PCR	15
TRIB1	H. sapiens	Reporter assay; qRT-PCR	15
UBAP2	H. sapiens	Reporter assay; qRT-PCR	15
VAV3	H. sapiens	Reporter assay	71
XPO6	H. sapiens	Reporter assay; qRT-PCR	15
Non-functional miRNA-target interactions (Negative samples)			
MSN	H. sapiens	Reporter assay	71
B2m	M. musculus	Reporter assay	This study
Afp	M. musculus	Reporter assay	This study
Ccl2	M. musculus	Reporter assay	This study
Csf3r	M. musculus	Reporter assay	This study
Ctgf	M. musculus	Reporter assay	This study
Cxcl13	M. musculus	Reporter assay	This study
Cyp2b13	M. musculus	Reporter assay	This study
Dbp	M. musculus	Reporter assay	This study
Igf2	M. musculus	Reporter assay	This study
Il1b	M. musculus	Reporter assay	This study
Jun	M. musculus	Reporter assay	This study
Per1	M. musculus	Reporter assay	This study
Ccnd1	M. musculus	Reporter assay	8
Irf6	M. musculus	Reporter assay	8
Socs2	M. musculus	Reporter assay	8
Rbl2	M. musculus	Reporter assay	8
Camk2b	M. musculus	Reporter assay	8
Tmem20	M. musculus	Reporter assay	8
Gapdh	M. musculus	Reporter assay	38

H. sapiens, Homo sapiens; M. musculus, Mus musculus;

Supplemental Table 8. Performance comparisons of miRNA target prediction tools

		Sensitivity	Specificity	Accuracy	PERF*
Performance of each tool	miRanda	91.3%	38.9%	81.6%	0.355
	TargetScanS	58.8%	77.8%	62.2%	0.457
	RNAhybrid	68.8%	66.7%	68.4%	0.459
	PITA	85.0%	44.4%	77.6%	0.377
Performance of integrated tools (This study)	At least 3 tools	77.5%	72.2%	76.5%	0.560

***PERF (Performance) = Sensitivity x Specificity**

Supplemental Table 9. Nucleotide sequences of the PCR cloning primers for the 3'UTR reporter constructs

Gene	Primers	sequence
Afp	forward	CTCCGAGTCCAGAAGGAAGAGTGGAC
	reverse	GCGGCCGCAGACTAGGAGAAGAGAAATAGTT
Aldoa	forward	CTCGAGCCAGAGCTGAACTAAGGC
	reverse	GCGGCCGCCTTAAATAGTTGTTTATTGGC
Alpl	forward	CTCGAGCAAGCCCGCAATGGAC
	reverse	GCGGCCGCTCCAAACAGGAGAGCC
B2m	forward	CTCGAGCTCTGAAGATTCATTTGAACCT
	reverse	GCGGCCGCGCTAAGCATTGGGCAC
Cs	forward	CTCGAGGGAATGACCAGCCTCT
	reverse	GCGGCCGCCATCCTGAAGTCTGCATC
Ctgf	forward	CTCGAGGCATGTGTCCTCCACT
	reverse	GCGGCCGCATCGGACCTTACCCTGA
Igf2	forward	CTCGAGGACCTCCTCTTGAGCAG
	reverse	GCGGCCGCTGTGGACAGGTGCTTAGA
Jun	forward	CTCGAGGCTGAGTGCCCAATATAC
	reverse	GCGGCCGCAGAGAAAGCTCACC
Klf6	forward	CTCGAGCTGGCAAGACACGTTC
	reverse	GCGGCCGCCTTTCAGTATTACCAACAGATAGC
Prom1	forward	CTCGAGTTTGGAGCTACCTGCG
	reverse	GCGGCCGCGAACGTAATGCCCATTCT
Sox4	forward	CTCGAGTAGAGCTGGCCTGGAAC
	reverse	GCGGCCGCCTTGACCATGAGGCAAAAT

Supplemental Table 10. RT-PCR primers used in mutagenesis reactions

Gene		sequence
Klf6-M1	forward	CCTTCTATTTTGTAGCGCGCACATGCAAAATGATCTTG
	reverse	CAAGATCATTTTGCATGTGCGCGCTGCAAAATAGAAGG
Klf6-M2	forward	CATACACACACGCGCGCGCAGGCTGTATTTATTATG
	reverse	CATAATAAATACAGCCTGCGCGCGCGTGTGTGTATG

References

63. Gutierrez-Ruiz, M.C. & Gomez-Quiroz, L.E. Liver fibrosis: searching for cell model answers. *Liver Int* **27**, 434-9 (2007).
64. Bosselut, N. et al. Distinct proteomic features of two fibrogenic liver cell populations: hepatic stellate cells and portal myofibroblasts. *Proteomics* **10**, 1017-28 (2010).
65. Bai, S. et al. MicroRNA-122 inhibits tumorigenic properties of hepatocellular carcinoma cells and sensitizes these cells to sorafenib. *J Biol Chem* **284**, 32015-27 (2009).
66. Fabani, M.M. & Gait, M.J. miR-122 targeting with LNA/2'-O-methyl oligonucleotide mixmers, peptide nucleic acids (PNA), and PNA-peptide conjugates. *RNA* **14**, 336-46 (2008).
67. Shan, Y., Zheng, J., Lambrecht, R.W. & Bonkovsky, H.L. Reciprocal effects of micro-RNA-122 on expression of heme oxygenase-1 and hepatitis C virus genes in human hepatocytes. *Gastroenterology* **133**, 1166-74 (2007).
68. Lin, C.J., Gong, H.Y., Tseng, H.C., Wang, W.L. & Wu, J.L. miR-122 targets an anti-apoptotic gene, Bcl-w, in human hepatocellular carcinoma cell lines. *Biochem Biophys Res Commun* **375**, 315-20 (2008).
69. Gramantieri, L. et al. Cyclin G1 is a target of miR-122a, a microRNA frequently down-regulated in human hepatocellular carcinoma. *Cancer Res* **67**, 6092-9 (2007).
70. Kojima, S., Gatfield, D., Esau, C.C. & Green, C.B. MicroRNA-122 modulates the rhythmic expression profile of the circadian deadenylase Nocturnin in mouse liver. *PLoS One* **5**, e11264 (2010).
71. Xu, H. et al. Liver-enriched transcription factors regulate microRNA-122 that targets CUTL1 during liver development. *Hepatology* **52**, 1431-42 (2010).
72. Song, K.H., Li, T., Owsley, E. & Chiang, J.Y. A putative role of micro RNA in regulation of cholesterol 7alpha-hydroxylase expression in human hepatocytes. *J Lipid Res* **51**, 2223-33 (2010)
73. Akinc, A. et al. A combinatorial library of lipid-like materials for delivery of RNAi therapeutics. *Nat Biotechnol* **26**, 561-9 (2008).